INTERNATIONAL ATOMIC ENERGY AGENCY
UNITED NATIONS EDUCATIONAL, SCIENTIFIC AND CULTURAL ORGANIZATION

INTERNATIONAL CENTRE FOR THEORETICAL PHYSICS
34100 TRIESTE (ITALY) - P.O.B. 586 - MIRAMARE - STRADA COSTIERA 11 - TELEPHONE: 2240-1
CABLE: CENTRATOM - TELEX 460392 - I

SMR/388 - 50

SPRING COLLEGE IN MATERIALS SCIENCE ON 'CERAMICS AND COMPOSITE MATERIALS'
(17 April - 26 May 1989)

STRUCTURAL PROPERTIES OF OXIDE SUPERCONDUCTORS
(Background Material)

C.N.R. RAO
Indian Institute of Science
Solid State and Structural Chemistry Unit
560 012 Bangalore
India

---

of an alkyne complex into a dialkylidyne complex either from theoretical analysis on cobalt or from experimental evidence on rhodium and iridium. If Ru, Co, Ir, and Mo behave differently than Ni, Pd, (W), it may be, as pointed out by Saillard et al.[58] from the plot of relative electron distribution as a function of electron count, that, at the right side of the transition series, surfaces should be negative relative to the bulk, and at the left side of the transition series, surfaces should be positive.

Our general conclusions will then be that possible surface intermediates in alkane reactions on metallic catalysts have only indirect proof in their support; however, they account for many experimental facts. We proposed an agostic precursor species which initiates the formation of σ-alkyl or carbene species to explain (a) the bond-shift, the cyclic, and the hydrogenolysis reactions; (b) less dehydrogenated species on the surface,[35,45] in agreement with the kinetic model proposed by Frennet et al.;[31] (c) dicarbyne mobility on the surface as proposed in ref 29. The $\alpha\alpha\gamma$ triadsorbed species proposed by Leclercq et al.[60] and Anderson et al.[26,27,34] Furthermore, the surface reconstructions of platinum single crystals by hydrogen correlated to change in the selectivity in isomerization and hydrogenolysis reactions reinforce the proposed agostic precursor.

More generally, our proposal for an agostic precursor species has the advantage of simplifying the interpretation of the different reaction mechanisms for isomerization and hydrogenolysis via a limited number of precursor species. It also allows us to account for the first steps of adsorption as well on platinum, palladium, and iridium catalysts as on bimetallic or alloy catalysts and agrees very well with the kinetic model proposed by Frennet,[30] where a reactive adsorption step occurs, followed by reactive surface dehydrogenation steps without any release of the sites occupied by adsorbed hydrogen.

We are grateful to Dr. David Godbey, Department of the Navy, Naval Research Laboratory, Washington, DC 20375, for extensive discussions.

(60) Leclercq, G.; Leclercq, L.; Maurel, R. *J. Catal.* 1977, *50*, 87.

Structural Aspects of High-Temperature Cuprate Superconductors[†]

C. N. R. Rao*

Solid State and Structural Chemistry Unit, Indian Institute of Science, Bangalore 560012, India

B. Raveau

Laboratoire de Cristallographie et Sciences des Materiaux, Institut des Sciences de la Matiere et du Rayonnement (ISMRa Campus2), Bd du Marechal Juin, 14032 Caen Cedex, France

Received September 16, 1988 (Revised Manuscript Received January 4, 1989)

Introduction

High-temperature superconductivity constitutes the most sensational discovery of recent times. Since these new superconductors are complex metal oxides, chemistry has had a big role to play in the investigations. For the first time, stoichiometry, structure, bonding, and such chemical factors have formed central themes in superconductivity, an area traditionally dominated by physicists. These oxide superconductors have given a big boost to solid-state chemistry.

The first group of high-temperature superconductors discovered[1] were oxides of the type $La_{2-x}(Ca,Sr,Ba)_xCuO_4$ with T_c values in the 25–40-K range, soon followed by the so-called 123 oxides of the general formula $LnBa_2Cu_3O_7$ (Ln = Y, Nd, Sm, Eu, Gd, Dy, Ho, Er, Tm, or Yb) with T_c values in the 90-K region. The chemistry of these two classes of oxide superconductors has been reviewed recently.[2-7] The discovery of ma-

C. N. R. Rao (born 1934) obtained his M.Sc. degree from Banaras, D.Sc. degree from Mysore, and Ph.D. and D.Sc. (honoris causa) degrees from Purdue. He is the founder–Chairman of the Solid State and Structural Chemistry Unit at the Indian Institute of Science, where he continues as a Professor and Director. He is a Fellow of the Royal Society, London, and a foreign honorary member of the American Academy of Sciences and Arts as well as of the Polish and U.S.S.R. science academies. He is a centennial foreign fellow of the American Chemical Society. His main research interests are solid-state chemistry of metal oxides, surface science, and chemical spectroscopy.

B. Raveau (born 1940) studied engineering as an undergraduate and obtained his doctorate degree in chemistry at Caen in 1966. He soon became professor at Caen, where he heads a flourishing school in solid-state chemistry. He now has an active team working on superconductivity and is collaborating with industry in developing devices. His main areas of interest are phosphate–bronze alloys, mixed-valent copper oxides, and applied solid-state chemistry.

[†] Contribution no. 575 from the Solid State & Structural Chemistry Unit.

(1) Bednorz, J. G.; Müller, K. A. *Z. Phys. B: Condens. Matter* 1986, *64*, 189.

(2) *Chemistry of High-Temperature Superconductors*; Nelson, D. L., Whittingham, M. S., George, T. F., Eds.; ACS Symposium Series 351; American Chemical Society: Washington, DC, 1987.

(3) Williams, J. M.; Beno, M. A.; Carlson, K. D.; Geiser, U.; Kao, H. C. I.; Kini, A. M.; Porter, L. C.; Schultz, A. J.; Thorn, R. J.; Wang, H. H.; Whangbo, M. H.; Evain, M. *Acc. Chem. Res.* 1988, *21*, 1.

(4) Holland, G. F.; Stacy, A. M. *Acc. Chem. Res.* 1988, *21*, 8.

(5) Rao, C. N. R. *J. Solid State Chem.* 1988, *74*, 147. Rao, C. N. R. *Mod. Phys. Lett. B* 1988, 2, 1217.

(6) *Chemistry of Oxide Superconductors*; Rao, C. N. R., Ed.; Blackwell Sci. Publns: Oxford, 1988. Also see: Chemical and Structural Aspects of High-Temperature Superconductors. In *Progress in High-Temperature Superconductivity*; Rao, C. N. R., Ed.; World Scientific: Singapore, 1988; Vol. VII.

(7) Raveau, B., et al. *Caen High T_c Superconductors*; University of Caen, France: Vols. I–IV.

0001-4842/89/0122-0106$01.50/0

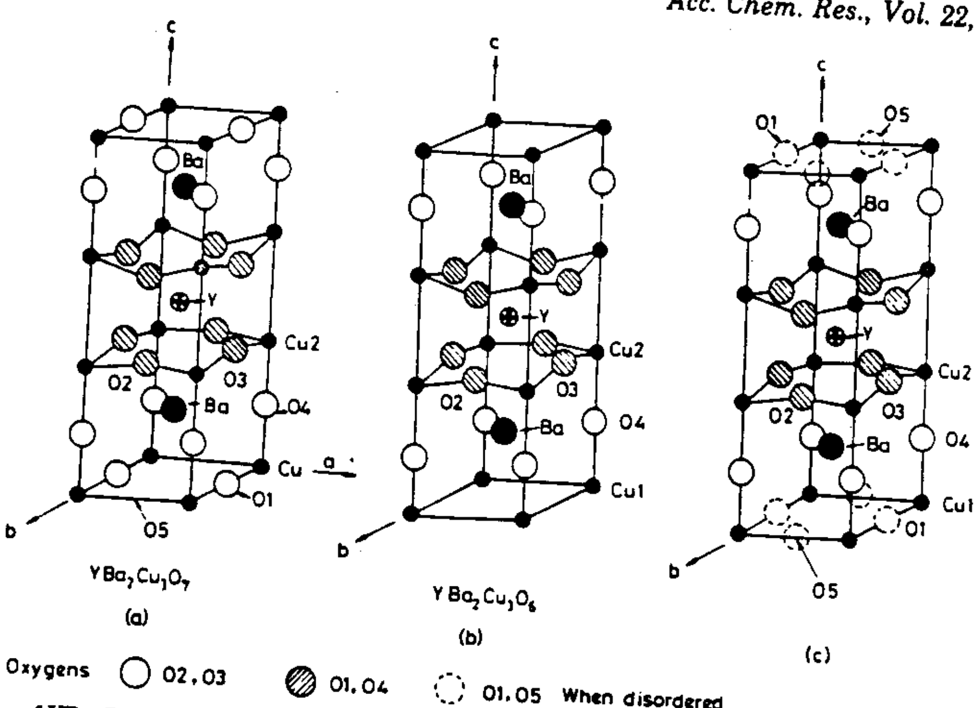

Figure 1. Structure of $YBa_2Cu_3O_{7-\delta}$: (a) $\delta = 0.0$, orthorhombic with oxygens ordered on O1 sites; (b) $\delta = 1.0$, tetragonal with fully depleted O1 sites; (c) disordered structure where both O1 and O5 sites are occupied.

terials with superconductivity above the liquid-nitrogen temperature has raised much hope and has prompted intensive search for new classes of oxides with still higher superconducting transition temperatures. Two new series of layered oxides belonging to the Bi–Ca–Sr–Cu–O and Tl–Ca–Ba–Cu–O systems and possessing the general formula $A_2Ca_{n+1-x}B_xCu_nO_{2n+4}$ where A = Bi or Tl and B = Sr or Ba have been found to exhibit superconductivity between 60 and 125 K.[6-18] A few members of the series (n = 1–3) of oxides have been characterized adequately, although there has been some difficulty in obtaining pure phases, especially in the bismuth cuprate system. The $TlCa_{n-1}Ba_2Cu_nO_{2n+3}$ series of superconductors containing only a single Tl–O layer (compared to two Tl–O layers of the earlier series) is also known.[15,18-20] Recently, superconducting lead cuprates of the type $PbASr_2Cu_3O_{8+\delta}$ (A = Ln or Ln + Ca) have been discovered.[21]

It is noteworthy that all the high-T_c cuprates possess perovskite-related structures with covalent Cu–O bonds and exhibit some common features. In this Account, we present some of the significant structure–property relations in the various cuprate superconductors, distilled from the recent literature and substantially based on our own contributions to this area. In view of the immense literature on the subject, we shall cite only a few of the key references. We shall first present the essential features of the $La_{2-x}(Ca,Sr,Ba)_xCuO_4$ and $LnBa_2Cu_3O_7$ systems[22] and then discuss the bismuth and thallium cuprate superconductors. We shall then highlight the structural relationships as well as the commonalities among the different superconducting cuprates and examine the states of copper and oxygen ions in the cuprates. We shall point out how oxygen holes play a role in the superconductivity. The involvement of oxygen holes in determining the properties of metal oxides constitutes an important new idea that needs to be explored further. That the oxygen holds the key to the superconductivity of oxides is also substantiated by the discovery of relatively high T_c (~30 K) superconductivity in oxides such as $Ba_{1-x}K_xBiO_3$ not containing copper.[23]

Some Important Features of $La_{2-x}(Ca,Sr,Ba)_xCuO_4$ and $LnBa_2Cu_3O_7$[22]

$La_{2-x}Ba_x(Sr_x)CuO_4$ compounds have the quasi-two-dimensional K_2NiF_4 structure with tetragonally elongated Cu–oxygen octahedra; the Cu ions can interact

---

(8) Maeda, H.; Tanaka, Y.; Fukutomi, M.; Asano, T. *Jpn. J. Appl. Phys.* 1988, *27*, L209.

(9) Hervieu, M.; Michel, C.; Domenges, B.; Laliguant, Y.; Lebail, A.; Feray, G.; Raveau, B. *Mod. Phys. Lett. B* 1988, *2*, 491, 835.

(10) Hazen, R. M.; Drewitt, C. T.; Angel, R. J.; Ross, N. L.; Finger, L. W.; Hadidiacos, C. G.; Velden, D. R.; Heaney, P. J.; Hor, P. H.; Meng, R. L.; Sun, Y. Y.; Wang, Y. Q.; Xue, Y. Y.; Huang, Z. J.; Gao, L.; Bechtold, J.; Chu, C. W. *Phys. Rev. Lett.* 1988, *60*, 1174.

(11) Subramanian, M. A.; Torardi, C. C.; Calabrese, J. C.; Gopalakrishnan, J.; Morrissey, J. J.; Askew, T. R.; Flippen, R. B.; Chowdhry, U.; Sleight, A. W. *Science* 1988, *239*, 1015.

(12) Rao, C. N. R.; Ganapathi, L.; Vijayaraghavan, R.; Rao, G. R.; Murthy, K.; Mohan Ram, R. A. *Physica C* 1988, *156*, 827; *J. Solid State Chem.*, to be published.

(13) Sheng, Z. Z.; Hermann, A. M. *Nature* 1988, *332*, 55, 138. Sheng, Z. Z.; Hermann, A. M.; Ali, A. E.; Almasan, C.; Estrada, J.; Datta, T. *Phys. Rev. Lett.* 1988, *74*, 428.

(14) Maignan, A.; Michel, C.; Hervieu, M.; Martin, C.; Groult, D.; Raveau, B. *Mod. Phys. Lett. B* 1988, *2*, 681.

(15) Martin, C.; Michel, C.; Maignan, A.; Hervieu, M.; Raveau, B. *C. R. Acad. Sci., Ser. 2* 1988, *307*, 27.

(16) Parkin, S. S. P.; Lee, V. Y.; Engler, E. M.; Nazzal, A. I.; Huang, J. C.; Gorman, G.; Savoy, R.; Beyers, R. *Phys. Rev. Lett.* 1988, *60*, 2539.

(17) Ganguli, A. K.; Nanjundaswamy, K. S.; Subbanna, G. N.; Umarji, A. M.; Bhat, S. V.; Rao, C. N. R. *Solid State Commun.* 1988, *67*, 39.

(18) Ganguli, A. K.; Nanjundaswamy, K. S.; Subbanna, G. N.; Rajumon, M. K.; Sarma, D. D.; Rao, C. N. R. *Mod. Phys. Lett. B* 1988, *2*, 1169.

(19) Hervieu, M.; Maignan, A.; Martin, C.; Michel, C.; Provost, J.; Raveau, B. *J. Solid State Chem.* 1988, *75*, 212.

(20) Parkin, S. S. P.; Lee, V. Y.; Nazzal, A. I.; Savoy, R.; Beyers, R.; La Placa, S. I. *Phys. Rev. Lett.* 1988, *61*, 750.

(21) Cava, R. J.; Batlogg, B.; Krajewski, J. J.; Rupp, L. W.; Schneemeyer, L. F.; Siegrist, T.; van Dover, R. B.; Marsh, P.; Peck, W. F., Jr.; Gallagher, P. K.; Glarum, S. H.; Marshall, J. H.; Farrow, R. C.; Waszczak, J. V.; Hull, R.; Trevor, P. *Nature* 1988, *336*, 221.

(22) We shall not cite all the references to the original literature here. These can be found from ref 2–7, which review these materials. Some of the unpublished work from our laboratories has been included without specific references.

(23) Cava, R. J.; Batlogg, B.; Krajewski, J. J.; Farrow, R.; Rupp, L. W.; White, A. E.; Short, K.; Peck, W. F.; Kometani, T. *Nature* 1988, *332*, 814.

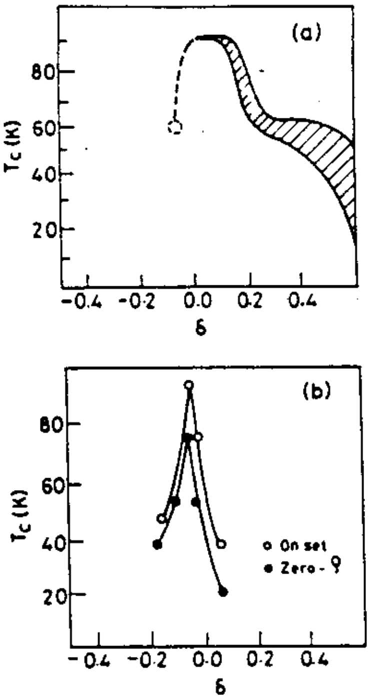

Figure 2. Variation of T_c with δ in (a) $YBa_2Cu_3O_{7-\delta}$ and (b) $LaBa_2Cu_3O_{7-\delta}$. Shaded region includes data from different sources.

only in the *ab* plane. These oxides have a tetragonal structure at room temperature when $x > 0.05$ and become orthorhombic around 180 K, well above the superconducting transition temperature (25–40 K). T_c in these oxides shows a maximum around a specific value of x (~0.15 and 0.2 respectively in the case of Ba and Sr), around which compositions certain structural parameters also seem to show anomalous features. Parent La_2CuO_4 ($x = 0$) is itself orthorhombic and becomes superconducting ($T_c \sim$ 30–40 K) when it has an oxygen excess or a lanthanum deficiency. The La ion in $La_{2-x}Ba_x(Sr_x)CuO_4$ can be replaced by rare earth ions such as Pr, Nd, Eu, and Gd up to a point (<10%) without losing superconductivity, although T_c is generally lowered. Substitution of Cu partly by Ni and Zn also lowers the T_c.

$YBa_2Cu_3O_{7-\delta}$ and related 123 oxides are orthorhombic (Figure 1), by virtue of the preferential population of the O1 sites (along the *b* axis) giving rise to Cu–O chains. A disordered orthorhombic structure can result if both the O1 and O5 sites are occupied (but unequally). A tetragonal structure results if the O1 oxygens are depleted extensively or the O1 and O5 sites are equally occupied. The tetragonal–orthorhombic transition is responsible for the formation of twins; across the twin boundary, the Cu–O chain direction is rotated by 90°. The orthorhombic structure of $YBa_2Cu_3O_{7-\delta}$ continues up to $\delta \approx 0.6$ when the structure becomes tetragonal; $YBa_2Cu_3O_6$ is tetragonal and nonsuperconducting. The T_c of orthorhombic $YBa_2Cu_3O_{7-\delta}$ shows an interesting variation with δ. The T_c is ~90 K up to $\delta \approx 0.20$; there is a plateau in T_c (55 ± 5 K) in the δ range of 0.20–0.40 (Figure 2). The material becomes nonsuperconducting at $\delta \approx 0.6$. The orthorhombic structure can be extended to higher values of δ by low-temperature gettering, but the T_c values of such samples are rather low (≲40 K). Since the structure in the plateau region is orthorhombic, the possible occurrence of oxygen vacancy ordering has to be examined. While some evidence for vacancy ordering has been found in electron-diffraction patterns, it seems to depend on the method of preparation of the samples. Such compositions can be mixtures of orthorhombic O_7 and tetragonal O_6 structures. More interestingly, intergrowths of O_7 and O_6 structures can occur in compositions with $\delta \geq 0.50$. Occurrence of superconductivity ($T_c \lesssim 45$ K) in these compositions (especially $\delta \simeq 0.5$) is better explained by intergrowths of domains that are alternately superconducting and insulating according to the formulation $YBa_2(Cu_2^{2+}Cu^{3+}O_7)_{1-x}(Cu_2^{2+}Cu^{1+}O_6)_x$.[24] In Figure 3 we illustrate the nature of the intergrowth structure of O_7 and O_6 units suggested by electron microscopic observations.

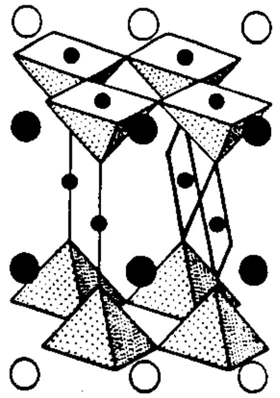

Figure 3. Intergrowths of superconducting "O_7" domains (CuO_4 square-planar groups) and insulating "O_6" domains (Cu in 2-fold coordination).

Unlike in $YBa_2Cu_3O_{7-\delta}$, $LaBa_2Cu_3O_{7-\delta}$ becomes tetragonal for relatively small deviations from stoichiometry ($|\delta| < 0.1$). Oxygen-excess $LaBa_2Cu_3O_{7-\delta}$ samples are more readily obtained than in the yttrium system, but these are almost always tetragonal and nonsuperconducting. High T_c (~77 K) in $LaBa_2Cu_3O_{7-\delta}$ is found only when $\delta \approx 0.0$ (Figure 2), at which composition the structure is orthorhombic.[6,25] The sensitivity of T_c to δ in $LnBa_2Cu_3O_7$ depends on the Ln (rare earth) ion. A plateau at lower T_c (~50 K) is seen for $\delta > 0.2$ when Ln = Gd or Dy as well, but the orthorhombic structure in this δ region is different from that in the 90 K T_c region ($b = c/3$). All $LnBa_2Cu_3O_7$ compounds become tetragonal above a certain temperature (e.g.: La, 590 K; Y, 970 K). The larger Ln ions can readily interchange sites with Ba, unlike the smaller ions. This is also true of the more general $Ln_{3-x}Ba_{3+x}Cu_6O_{14+\nu}$ family of which the 123 oxides are the $x = 1$ members. In the 336 family, the structural dependence (orthorhombic/tetragonal) on x depends on the Ln ion; oxygen-excess compositions of the 336 family generally possess tetragonal structures.[6,26]

A variety of studies have been carried out to investigate the effect of substituting Y, Ba, or Cu by other metal ions. The Cu ion in $YBa_2Cu_3O_7$ can be replaced by cations such as Zn and Fe, and these substitutions generally tend to give rise to tetragonal structures accompanied by changes in oxygen stoichiometry and lower T_c values.[27] While most high-T_c (~90 K) 123

[24] Raveau, B.; Michel, C.; Hervieu, M.; Provost, J. *Physica C* **1988**, *153–155*, 3.

[25] Ganapathi, L.; Ganguli, A. K.; Mohan Ram, R. A.; Rao, C. N. R. *J. Solid State Chem.* **1988**, *73*, 593; *J. Solid State Chem.* **1988**, *76*, 235.

[26] Umarji, A. M.; Somasundaram, P.; Ganapathi, L.; Rao, C. N. R. *Solid State Commun.* **1988**, *66*, 177.

[27] See, for example: Bordet, P.; Hodeau, J. L.; Strobel, P.; Marezio, M.; Santoro, A. *Solid State Commun.* **1988**, *66*, 435.

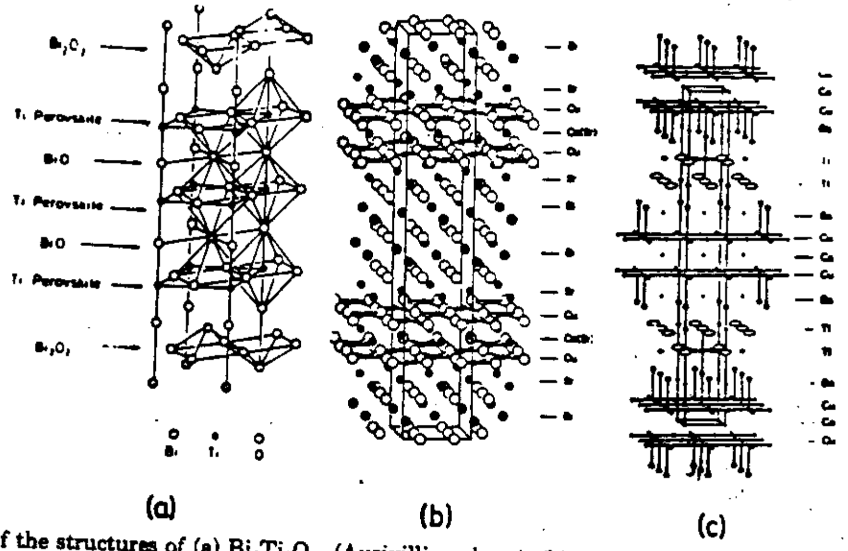

Figure 4. Comparison of the structures of (a) $Bi_4Ti_3O_{12}$ (Aurivillius phase), (b) $Bi_2(Ca,Sr)_3Cu_2O_8$ (after Subramanian et al.[11]), and (c) $Tl_2CaBa_2Cu_2O_8$ (after Subramanian et al.[34]).

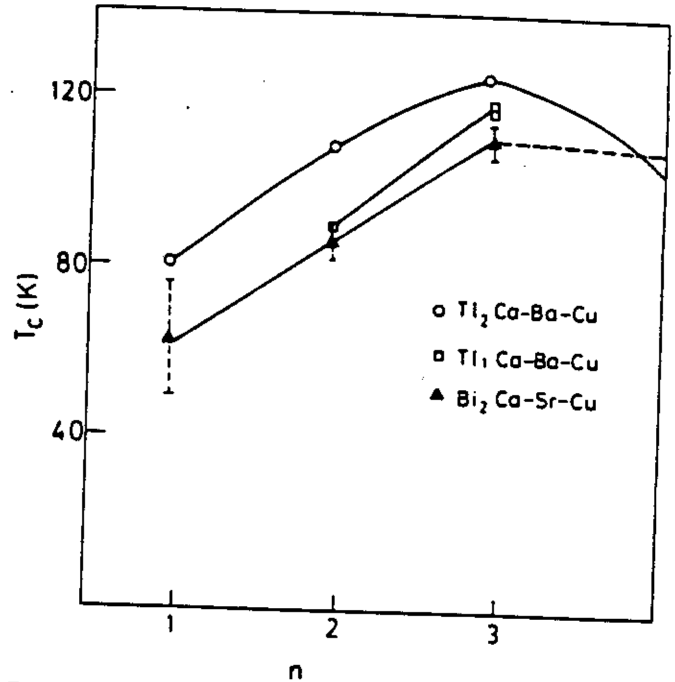

Figure 5. Variation of T_c in Bi and Tl cuprates with the number of Cu–O layers, *n*.

oxides are orthorhombic, certain tetragonal 123 compositions with high T_c values have been prepared.[28,29] Orthorhombicity is not a necessary criterion for high T_c. The tetragonal superconducting samples, however, show orthorhombic microdomains in electron micrographs. $PrBa_2Cu_3O_{7-\delta}$ is orthorhombic, but not superconducting.[30]

When Ba in $YBa_2Cu_3O_7$ is progressively replaced by Sr, the T_c is lowered. Substitution of Y by Pr has a similar effect until superconductivity is lost at ~60% Pr. In $YBa_{2-x}La_xCu_3O_{7-\delta}$, the structure becomes tetragonal with increase in *x* and the T_c of the orthorhombic phase decreases with increase in *x*. The lability of oxygen is reduced by partial substitution of Ba by La, a factor that may be useful in materials processing.[31] In oxides such as $GdBa_2Cu_3O_7$, superconductivity coexists with magnetism.[32]

Bi–Ca–Sr–Cu–O and Tl–Ca–Ba–Cu–O Systems[6–20,33–42]

After the initial report of superconductivity (maximum $T_c \approx 22$ K) in $Bi_2Sr_2CuO_{6+\delta}$ by Michel et al.,[33] Maeda et al.[8] reported high T_c with onset in the 100 K region in a Bi–Ca–Sr–Cu–O composition. Since then, several compositions of the Bi–Ca–Sr–Cu–O system belonging to the $Bi_2(Ca,Sr)_{n+1}Cu_nO_{2n+4}$ series have been investigated widely. The $n = 2$ member of this series, $Bi_2(Ca,Sr)_3Cu_2O_{8+\delta}$, with zero-resistance T_c of ~90 K, has been characterized by several workers both in polycrystalline and single-crystal forms. The exact composition of the phase, however, seems to vary from one laboratory to another. The $n = 2$ member seems to be the most stable phase in this series. The bismuth cuprates are orthorhombic and have structures somewhat similar to those of the Aurivillius family of oxides,

(28) Langen, J.; Veit, M.; Galffy, M.; Jostarndt, H. D.; Erle, A.; Blumenröder, S.; Schmidt, H.; Zirngiebl, E. *Solid State Commun.* 1988, *65*, 973.

(29) Maeno, J.; Fujita, T. *Physica C* 1988, *153–155*, 1105. Also see: Jing, J.; Beig, J.; Engelmann, H.; Hsia, Y.; Gonser, Y.; Gütlich, P.; Jakobi, R. *Solid State Commun.* 1988, *66*, 727.

(30) Ganguli, A. K.; Rao, C. N. R. *Z. Phys. B: Condens. Matter*, in press.

(31) Somasundaram, P.; Nanjundaswamy, K. S.; Umarji, A. M.; Rao, C. N. R. *Mater. Res. Bull.* 1988, *23*, 1139. Manthiram, A.; Tang, X. X.; Goodenough, J. B. *Phys. Rev. B* 1988, *37*, 3734.

(32) Dunlap, B. D.; Slaski, M.; Hinks, D. G.; Soderholm, L.; Beno, M.; Zhang, K.; Segre, C.; Crabtree, G. W.; Kwok, W. K.; Malik, S. K.; Schuller, I. K.; Jorgensen, J. D.; Sungila, Z. *J. Magn. Magn. Mater.* 1987, *68*, L139.

(33) Michel, C.; Hervieu, M.; Borel, M. M.; Grandin, A.; Deslandes, F.; Provost, J.; Raveau, B. *Z. Phys. B: Condens. Matter* 1987, *68*, 421.

(34) Subramanian, M. A.; Calabrese, J. C.; Torardi, C. C.; Gopalakrishnan, J.; Askew, T. R.; Flippen, R. B.; Morrissey, K. J.; Chowdhry, U.; Sleight, A. W. *Nature* 1988, *332*, 420.

(35) Torrardi, C. C.; Subramanian, M. A.; Calabrese, J. C.; Gopalakrishnan, J.; McCarron, E. M.; Morrissey, K. J.; Askew, T. R.; Flippen, R. B.; Chowdhry, U.; Sleight, A. W. *Phys. Rev. B* 1988, *38*, 225.

(36) Tarascon, J. M.; Le Page, Y.; Barboux, P.; Bagley, B. G.; Greene, L. H.; McKinnon, W. R.; Hull, G. W.; Girond, M.; Hwang, D. M. *Phys. Rev. B* 1988, *37*, 9382; *Phys. Rev. B* 1988, *38*, 2504.

(37) Tallon, J. L.; Buckley, R. G.; Gilberd, P. W.; Presland, M. R.; Brown, I. W. M.; Bowden, M. E.; Christian, L. A.; Goguel, R. *Nature* 1988, *333*, 153.

(38) Rao, C. N. R.; Thomas, J. M. *Acc. Chem. Res.* 1985, *18*, 113.

(39) Torrardi, C. C.; Subramanian, M. A.; Calabrese, J. C.; Gopalakrishnan, J.; Morrissey, K. J.; Askew, T. R.; Flippen, R. B.; Chowdhry, U.; Sleight, A. W. *Science* 1988, *240*, 631.

(40) Hervieu, M.; Maignan, A.; Martin, C.; Michel, C.; Provost, J.; Raveau, B. *Mod. Phys. Lett. B* 1988, 2, 1103.

(41) Ganguli, A. K.; Nanjundaswamy, K. S.; Rao, C. N. R. *Physica C* 1988, *156*, 788. Ganguli, A. K.; Nagarajan, R.; Nanjundaswamy, K. S.; Rao, C. N. R. *Mater. Res. Bull.*, in press.

(42) Hervieu, M.; Michel, C.; Maignan, A.; Martin, C.; Raveau, B. *J. Solid State Chem.* 1988, *74*, 428.

$(Bi_2O_2)^{2+}(A_{n-1}B_nO_{3n+1})^{2-}$. In Figure 4, we compare the structures of $Bi_4Ti_3O_{12}$ and $Bi_2(Ca,Sr)_3Cu_2O_8$, both of which have similar *c* parameters in the region of 30 Å. The main difference is that the cuprate does not have Bi_2O_2 layers, but instead has BiO layers separated by ~3.25 Å; cleavage between the two layers yields charge-neutral sections.[11] This is probably why the bismuth cuprates have mica-like morphology. The Cu coordination, although pyramidal, tends to be essentially square-planar in $Bi_2(Ca,Sr)_3Cu_2O_8$ and O_6.[35] Electron micrographs of Bi–Ca–Sr–Cu–O oxides clearly show evidence for modulation in the structure; superlattice structures are seen in the diffraction patterns. The micrographs also show the presence of extensive dislocations and intergrowths of different layered sequences.

While most workers have characterized the $n = 2$ member of the Bi–Ca–Sr–Cu–O system, there has been considerable difficulty in obtaining pure monophasic materials especially of the $n = 3$ member.[36] $Bi_2CaSrCuO_{6+\delta}$ ($n = 1$) has a T_c of 60 ± 20 K, the actual value depending on the Ca/Sr ratio. We find that starting Ca-rich compositions tend to yield more monophasic products. Initial reports of two T_c values around 80 and 110 K in some of the compositions as well as the occurrence of very low T_c in some others are clearly due to the presence of different phases. While very low T_c values could arise from $Bi_2Sr_2CuO_{6+\delta}$ and such phases, the ~110-K T_c is almost certainly due to the presence of a small proportion of the $n = 3$ member.[36] $Bi_2(Ca,Sr)_4Cu_3O_{10+\delta}$ (up to ~20%) in mixture with the $n = 2$ member shows a T_c of ~105 K.[37] Pure $n = 3$ member (T_c ~105–110 K) has been characterized recently; substitution of Bi by Pb (up to 25%) favors the formation of this phase.[12]

On the basis of the characterization of a variety of compositions of the Bi–Ca–Sr–Cu–O system, it appears that the T_c values of the $n = 1$, 2, and 3 members are around 60 ± 20, 85 ± 5, and 107 ± 3 K, respectively,[12] the orthorhombic *c* parameters being ~25, 31, and 37 Å, respectively. The T_c clearly increases with the number of Cu–O layers up to $n = 3$ (Figure 5). The $n = 4$ member, synthesized recently, has a T_c only slightly higher than that of the $n = 3$ member.[12] It appears that T_c does not increase with the number of CuO sheets beyond three. Attempts have been made to synthesize recurrent intergrowth structures,[38] involving a periodic arrangement of different layered phases at the unit-cell level. Unfortunately, it has not been possible to prepare such ordered intergrowth structures involving members of the $Bi_2(Ca,Sr)_{n+1}Cu_nO_{2n+4}$ series, unlike in the case of the Aurivillius family of bismuth oxides.[38]

Superconductivity in the Tl–Ca–Ba–Cu–O system was first reported by Sheng and Hermann.[13] These tetragonal oxides have the general formula $Tl_2Ca_{n-1}Ba_2Cu_nO_{2n+4}$. In this series, $TlBa_2CuO_6$, $Tl_2CaBa_2Cu_2O_8$, and $Tl_2Ca_2Ba_2Cu_3O_{10}$ corresponding to n = 1, 2, and 3 with *c* parameters of ~23, 29, and 36 Å respectively are known to show T_c values of around 80, 110, and 125 K. Structures of the Tl–Ca–Ba–Cu–O superconductors are similar to those of the Bi–Ca–Sr–Cu–O system. In Figure 4, we compare the structure of $Tl_2CaBa_2Cu_2O_8$ with that of $Bi_2(Ca,Sr)_3Cu_2O_8$. These thallium cuprates have essentially corner-sharing square-planar CuO_4, groups oriented to the (001) planes just as in the bismuth cuprates, but the copper–oxygen polyhedra are more distorted in the latter. There are no oxygen atoms between the Cu–O sheets. The Cu–O distance in $Tl_2Ca_{n-1}Ba_2Cu_nO_{2n+4}$ decreases with increase in n, accompanied by a small decrease in the *a* parameter; the intersheet Tl–O bonds are ~2.0 Å in length, and the separation between two Tl layers is 2.2 Å.[34,39] Crystals of the Tl cuprates are therefore difficult to cleave and are rod-shaped. Increasing the T_c in the Tl–Ca–Ba–Cu–O system to much higher temperatures by increasing n seems difficult since the $n = 4$ member has a T_c of 104 K.[40] Electron-diffraction patterns of the $n = 5$ member have been obtained, but the pure phase has not been isolated. Electron micrographs show defects and intergrowths of different sequences in the Tl cuprates as well.

The $n = 2$ and 3 members of the $TlCa_{n-1}Ba_2Cu_nO_{2n+3}$ series containing only one Tl–O layer have been isolated and characterized.[14,19–21] These oxides have T_c values lower than those of corresponding members of the $Tl_2Ca_{n-1}Ba_2Cu_nO_{2n+4}$ series (Figure 5), suggesting a role for the Tl layers. Recently, members of the $Tl_{1-x}Pb_x(Ca,Sr)_{n+1}Cu_nO_{2n+3}$ series of high-T_c superconductors have been characterized; substitution of Ca partly by Y in Tl and Bi cuprates lowers the T_c markedly.[41] $TlCa_{0.5}Ln_{0.5}Sr_2Cu_2O_y$ (Ln = Y or rare earth), however, represents a series of 1122-type superconductors (T_c ~ 90 K).

Structural Relationships in the Cuprates

A feature common to all the high-T_c cuprate superconductors is the high covalency of the Cu–O bonds and the two-dimensional character of the copper–oxygen framework closely related to that of the perovskites. Thus, $La_{2-x}(Ca,Sr,Ba)_xCuO_4$ as well as the Ba–Ca–Sr–Cu–O and Tl–Ca–Ba–Cu–O oxides can be considered to belong to the same structural family involving the intergrowth of multiple oxygen-deficient perovskite layers, $ACuO_{3-x}$, with rock-salt-type layers, AO, leading to the general formula $[ACuO_{3-x}]_n[AO]_{n'}$. $La_{2-x}M_xCuO_4$,[1,5] $Bi_2Sr_2CuO_6$,[33] and $Tl_2Ba_2CuO_6$[13] represent the $n = 1$ members formed of single perovskite layers according to the formulas $[La_{1-x}M_xCuO_{3-\delta}][La_{1-y}M_yO]$, $[SrCuO_3][(BiO)_2(SrO)]$, and $[BaCuO_3][(TlO)_2(BaO)]$. They differ from one another in the thickness of the rock-salt-type layer. One indeed observes single $[La_{1-y}M_yO]_\infty$ layers in La_2CuO_4-related oxides (Figure 6a) and triple rock-salt layers ($n' = 3$) in the other two oxides (Figure 6b) formed by a monolayer of [SrO] or [BaO] and bilayers of $[(BiO)_2]$ or $[(TlO)_2]$. The $n = 2$ members are represented by the three oxides $TlCaBa_2Cu_2O_7$,[18–20] $Bi_2CaSr_2Cu_2O_8$,[9,11,36,40] and $Tl_2CaBa_2Cu_2O_8$.[14,34,41] Here, the double oxygen-deficient perovskite layers ($n = 2$) are formed by two layers of corner-sharing CuO_5 pyramids interleaved with a plane of Ca ions leading to the formulas $[CaBa(CuO_{2.5}\square_{0.5})_2][(BaO)(TlO)]$, $[CaSr(CuO_{2.5}\square_{0.5})_2][(SrO)(BiO)_2]$, and $[CaBa(CuO_{2.5}\square_{0.5})_2][(BaO)(TlO)_2]$, where □ represents an oxygen vacancy. Thus, $TlCaBa_2Cu_2O_7$ (Figure 6c) exhibits a double rock-salt layer ($n' = 2$) formed of monolayers of (BaO) and (TlO) whereas triple rock-salt layers ($n' = 3$) formed of double $[(BiO)_2]$ or $[(TlO)_2]$ and a monolayer of [SrO] or [BaO] are present in $Bi_2CaSr_2Cu_2O_8$ and $Tl_2CaBa_2Cu_2O_8$ (Figure 6d). Triple oxygen-deficient perovskite layers

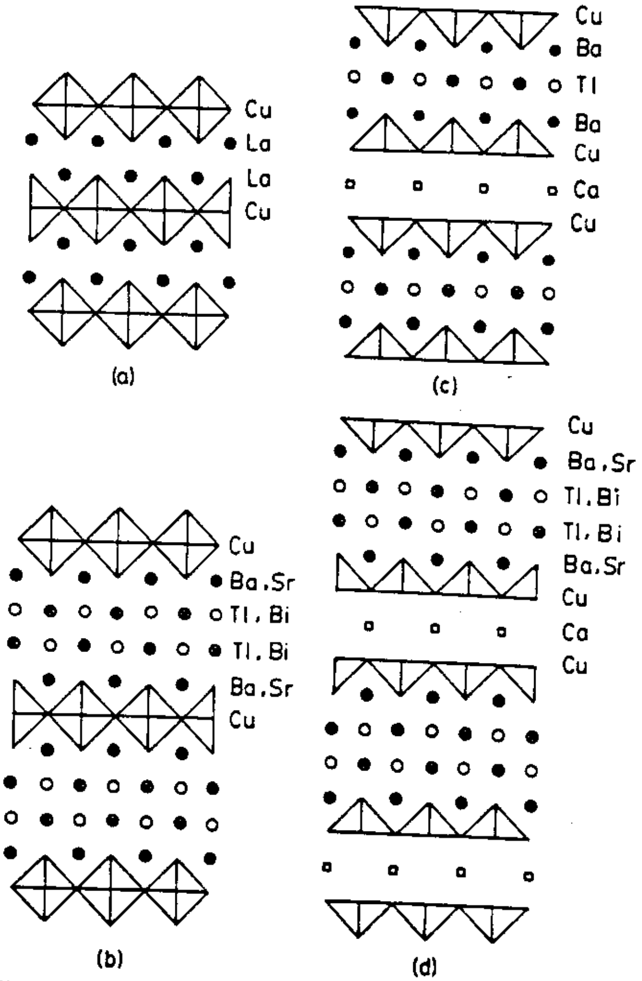

(a) (b) (c) (d)

Figure 6. Schematic representations of the structures of (a) La_2CuO_4-type oxides, (b) $Bi_2Sr_2CuO_6$ and $Tl_2Ba_2CuO_6$, (c) $TlCaBa_2Cu_2O_7$, and (d) $Bi_2CaSr_2Cu_2O_8$ and $Tl_2CaBa_2Cu_2O_8$. Oxygens are shown by open circles and Bi and Tl by circles with a cross.

(n = 3) are obtained in $TlCa_2Ba_2Cu_3O_9$,[14,20] $Tl_2Ca_2Ba_2Cu_3O_{10}$,[17,39,42] and $Bi_2Ca_2Sr_2Cu_3O_{10}$.[12,36,37] In these structures, the triple perovskite layer is formed by one layer of corner-sharing CuO_4 square-planar groups sandwiched by two layers of corner-sharing CuO_5 pyramids; two planes of Ca ions are interleaved between these layers. There are two rock-salt layers ($n' = 2$) in $TlCa_2Ba_2Cu_3O_9$ and three ($n' = 3$) in the other two oxides are illustrated in Figures 7a and 7b, respectively. Thus, the general formula of these three oxides can be written as $[BaCa_2(CuO_{2.5}\square_{0.5})_2(CuO_2\square)][(AO)_{1 or 2}(BO)]$, where B = Sr or Ba and A = Bi or Tl.

It is worth noting that the rock-salt layers, (TlO) and (BiO), are distorted compared to $La_{1-y}M_yO$ layers in La_2CuO_4-type oxides. The (TlO) layers are much less distorted than the (BiO) layers; the distance between two layers is indeed much larger in the latter. The $[CuO_2]_\infty$ layers of corner-sharing CuO_4 square-planar groups forming the basal planes of the octahedra or square pyramids are much less puckered in the La_2CuO_4-type oxides and in the thallium cuprates compared to the bismuth cuprates. This behavior of bismuth cuprates may be associated with the lone pair ($6s^2$) of bismuth, which may also be responsible for the modulation of the structure.

$YBa_2Cu_3O_7$ and related 123 oxides can be considered to constitute the $n' = 0$ members of the general structural class of oxygen-deficient perovskites described above. The ordering of oxygen and anionic vacancies in the perovskite framework (Figure 7c) leads to a layer structure that bears considerable similarity to the other cuprates. We can recognize similar layers of corner-sharing CuO_5 pyramids interleaved with planes of yttrium ions. The main difference in the 123 oxides is that two pyramidal layers are connected through rows of corner-sharing CuO_4 square-planar groups resulting in the formulation $[YBa(CuO_{2.5}\square_{0.5})_2][BaCuO_2\square]$. $YBa_2Cu_4O_8$ (124) with two CuO chains ($T_c \sim 80$ K) is also known.[43]

States of Copper and Oxygen

Superconducting $La_{2-x}M_xCuO_4$ and $LnBa_2Cu_3O_7$ would nominally be expected to contain a fair proportion of Cu^{3+} ions. Such a nominal Cu(II)–Cu(III) mixed valence has been considered to play an important role in the superconductivity of these oxides. Superconductivity in $YBa_2Cu_3O_{7-\delta}$ cannot be explained by taking into account the charge balance based on elementary chemical considerations alone. Thus, $YBa_2Cu_3O_{6.5}$, which should formally contain only Cu(II), should not be superconducting, but it shows a T_c of ~45 K. A possibility is that there is intergrowth of O_7 and O_6 domains as suggested earlier, requiring the presence of Cu(III), Cu(II), and Cu(I) states. What is interesting is that the T_c values of the La_2CuO_4-type oxides as well as $YBa_2Cu_3O_{7-\delta}$ show a proportional increase from 30 to 90 K with the nominal Cu^{3+}/Cu(total) ratio (Figure 8). However, this would not be the case in the Bi and Tl cuprates. We do not as yet fully understand the role of nonstoichiometry as well as of the TlO and BiO layers in the superconductivity of these cuprates.

Considerable effort has been made to understand the nature of copper and oxygen ions in the different cuprates since all the essential phenomena (magnetic properties and superconductivity) are confined to the CuO_2 sheets. It is well understood that localized Cu^{3+} ions cannot exist in the structures of these cuprates.[5,44] The excess positive charge (holes) is likely to be delocalized over the Cu–O framework as indicated by the metallic behavior of the cuprates. An important question that arises is whether the holes appear mainly on copper leading to the Cu(III) state (d^8 electron configuration) or whether they appear elsewhere. The answer from electron and X-ray spectroscopic studies is that all the excess holes end up as holes in the oxygen band or O^{1-} with $2p^5$ electronic configuration.

On the basis of X-ray absorption (Cu K or L edge) spectroscopy, many workers initially came to the conclusion that Cu^{3+} was present in $YBa_2Cu_3O_{6.9}$. Later measurements have, however, shown this not to be correct. The presence of a Cu^9-ligand hole state has been established by X-ray absorption spectroscopic studies; a 1s → 2p transition in the oxygen-edge spectrum confirms the presence of holes in the oxygen band, and this has also been verified by electron energy loss spectroscopy.[45–47]

---

(43) Marsh, P.; Fleming, R. M.; Mandich, M. L.; De Santolo, A. M.; Kwo, J.; Hong, M.; Miranda, L. J. M. *Nature* 1988, *334*, 141.

(44) Shafer, M. W.; Penney, T.; Olson, B. L. *Phys. Rev. B* 1987, *36*, 4047.

(45) Nücker, N.; Fink, J.; Fuggle, J. C.; Durham, P. J.; Temmerman, W. M. *Phys. Rev. B* 1988, *37*, 5158.

(46) Fuggle, J. C.; Weijs, P. J. W.; Schoorl, R.; Sawatzky, G. A.; Fink, J.; Nücker, N.; Durham, P. J.; Temmerman, W. M. *Phys. Rev. B* 1988, *37*, 123.

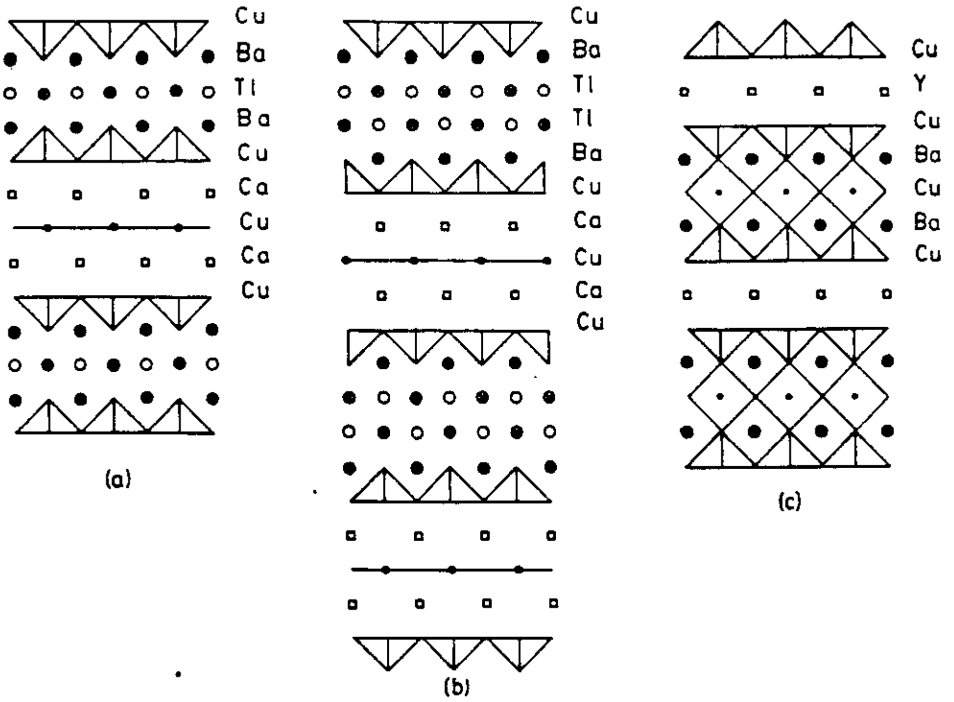

Figure 7. Schematic representations of (a) $TlCa_2Ba_2Cu_3O_9$, (b) $Tl_2Ca_2Ba_2Cu_3O_{10}$, and (c) $YBa_2Cu_3O_7$.

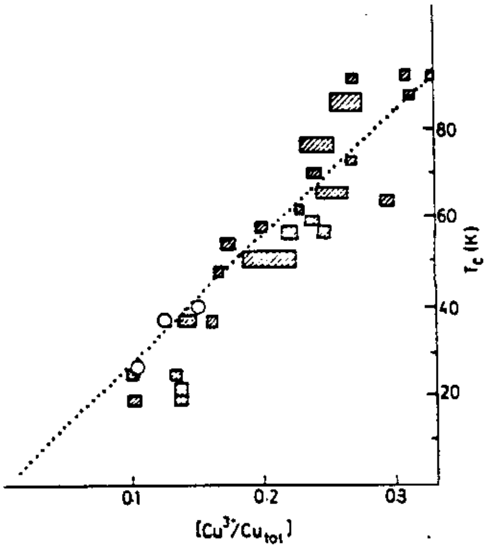

Figure 8. Variation of T_c with the nominal Cu^{3+}/Cu(total) ratio in $YBa_2Cu_3O_{7-\delta}$ (hatched rectangles) and $La_{2-x}Sr_xCuO_4$ (circles). The hatched rectangles include data of a number of workers.

We have investigated the nature of holes in the superconducting cuprates for some time by employing X-ray photoelectron (XP) and Auger electron spectroscopies.[48,49] Cu(2p) X-ray photoelectron and Cu L_3VV Auger spectra of $YBa_2Cu_3O_{6.9}$ as well as the Bi and Tl cuprates show the presence of only the Cu^{1+} and Cu^{2+} species in the ground state of these oxides, with no detectable amount of Cu^{3+}.

The O(1s) core-level spectra of the cuprates show the presence of features with binding energies of around 529, 531, and 533 eV, respectively.[48] The normally expected oxide species, O^{2-}, with the filled $2p^6$ configuration is associated with the 529-eV feature. The O^{1-} species (corresponding to the presence of a hole in the 2p band) is expected to have a higher binding energy than O^{2-}, but the position of this O(1s) feature is likely to be in the 529–531 region. Unfortunately, CO_3^{2-} and OH^-, which are almost always present in such oxides, give an intense peak around 531 eV. We, however, find an oxygen species with a binding energy of 533 eV which could be considered to be due to the dimerization of O^{1-} holes giving peroxide-like species. The proportion of the dimerized holes seems to increase substantially with decreasing temperature, and the phenomenon is reversible.[48,49] Although there is some uncertainty regarding the assignment of the 533-eV feature, it should be noted that a few other workers have recently assigned this to peroxide-like species.[50,51] The dimerized hole species could play an important role in the mechanism of superconductivity of these oxides. The presence of Cu^{1+} in the superconducting state of $YBa_2Cu_3O_{6.9}$ dictates that a considerable proportion of the oxygens be present in the hole state. Furthermore, the $d^{10}(Cu^{1+})$ state favors such oxygen holes.[52] It is interesting that Takura et al.[53] have recently correlated T_c of the cuprates with the [Cu–O] charge in the sheets. The charge, p, of $(Cu^{z+}\text{–}O^{m-})^p$ is determined by z and m; since $z \neq 3$, we can only have (a) $(Cu^{2+}O^{1-})^{1+}$, (b) $(Cu^{2+}O^{2-})^0$, and (c) $(Cu^{1+}O^{1-})^0$ species. It seems possible that the relative proportions of b and c will determine whether a particular oxide is superconducting or insulating for a given charge, p. It is noteworthy that the new superconducting lead cuprates[21] are required tc

---

(47) Bianconi, A.; Castellano, A. C.; De Santis, M.; Rudolf, P.; Lagarde, P.; Flank, A. M.; Marcelli, A. *Solid State Commun.* 1987, *63*, 1009; *Physica C* 1988, *153–155*, 1760.

(48) Sarma, D. D.; Rao, C. N. R. *Solid State Commun.* 1988, *65*, 47.

(49) Chakraverty, B. K.; Sarma, D. D.; Rao, C. N. R. *Physica C* 1988, *156*, 413.

(50) Chang, C. C.; Hegde, M. S.; Tarascon, J. M.; Venkatesan, T. Inam, A.; Wu, X. D.; Mc Lean, W. L. *Appl. Phys. Lett.* 1988, *53*, 2099

(51) Dai, Y.; Manthiram, A.; Campion, A.; Goodenough, J. B. *Phys Rev. B* 1988, *38*, 5091.

(52) Rao, C. N. R.; Hegde, M. S.; Ganguly, P.; Sarma, D. D. *J. Am Chem. Soc.* 1987, *109*, 6893.

(53) Takura, Y.; Torrance, J. B.; Huang, T. C.; Nazzal, A. I. *Phys. Rev B* 1988, *38*, 7156.

have a reasonable proportion of Cu^{1+} by virtue of their stoichiometry.

Concluding Remarks

We have attempted to point out the common structural features of the different families of cuprate superconductors. Besides being structurally related, we have shown that the cuprates are likely to have a common mechanism of superconductivity involving holes on oxygen. These holes seem to have mainly p_σ character.[49,54] Such holes may also be present in many other transition-metal oxides, especially those where the d electrons are itinerant.[49,52]

There are many chemical aspects of the oxide superconductors that are yet to be fully understood. Many new classes of oxides as well as other materials are yet to be explored. There are indications that many simple oxide systems may show superconductivity; other layered systems with Lu, Ga, In, etc., are yet to be explored. One possible strategy to follow would be to synthesize oxides or possibly other chalcogenides where anionic holes are favored. Chemically this means that we need to have systems with small anion to metal charge-transfer energy. Instead of being in a high oxide state, the metal would rather accept electrons from the anion (oxide) and create an anion (oxygen) hole. Besides oxides containing Bi and Pb, it would be worth investigating oxides containing Ni, V, Nb, Ti, Zr, Pd, and so on. There is also need to investigate three-dimensional oxide systems for superconductivity since $Ba_{1-x}K_xBiO_3$ has a T_c of ~30 K.[23] There is every hope that chemists will one day find a material with T_c close to room temperature. Their synthetic skills[55] will be of great value in this gold rush.

One of us (C.N.R.R.) acknowledges the Department of Science and Technology and the University Grants Commission for support of this research.

---

(54) Himpsel, F. J.; Chandrashekhar, G. V.; Shafer, M. W. *Phys. Rev. B* 1988, *38*, 11946.

(55) Rao, C. N. R.; Gopalakrishnan, J. *Acc. Chem. Res.* 1987, *20*, 228.

Physica C 156 (1988) 413–419
North-Holland, Amsterdam

CRUCIAL ROLE OF Cu^{1+} IONS AND OXYGEN HOLES (PEROXITONS) IN THE HIGH-TEMPERATURE SUPERCONDUCTIVITY OF CUPRATES

B.K. CHAKRAVERTY[#], D.D. SARMA and C.N.R. RAO[*]
Solid State & Structural Chemistry Unit, Indian Institute of Science, Bangalore 560 012, India

Received 5 August 1988

Recent spectroscopic data, especially based on electron spectroscopic measurements, have identified that the carriers in the normal state of the high-temperature superconducting cuprates are holes in the oxygen p-band rather than holes on copper in the form of Cu^{3+}. We show that these oxygen holes can form a special kind of singlet pair (which we designate peroxitons) composed of O^-–Cu^+–O^-) type species and essentially involving a resonating bond between the three sites. Bose condensation of these peroxitons as well as their effect on magnetic properties are discussed and it is shown that such oxygen holes are fundamental to the mechanism of superconductivity of the high T_c cuprates.

1. Introduction

Ever since the discovery [1] of the high-temperature oxide superconductors, there has been a flood of theoretical speculations, prominent amongst which has been the resonating valence bond (RVB) model [2,3] of positive charge carriers moving through the copper lattice sites in the copper–oxygen plane. The plethora of recent spectroscopic data [4–7] have drawn however the opposite conclusion that we have in these oxides, charge carriers which really are holes in the oxygen p-band (i.e. ligand holes rather than holes in the copper 3d-shell) and that these p-holes are somehow directly responsible for superconductivity in these oxides.

In this article, we shall first present some of the spectroscopic evidence for the oxygen holes and discuss the valence state of the copper ions. We shall then show the nature of pairing of these holes and address ourselves to the formation of the peroxiton pair. We shall discuss the relevance of the peroxitons to superconductivity and to magnetic properties of these oxides.

2. State of copper and oxygen

The archetype non-superconducting (actually, insulating) oxide of the family is stoichiometric La_2CuO_4, where every copper atom is in the Cu^{2+} state (d^1 i.e. 1 hole in the d-band) and oxygen is O^{2-} (p^0 i.e. no hole in the p-band). Since the d-hole resides in an antibonding $|d_{x^2-y^2}\rangle$ orbital, which is half-filled and ought to be metallic, it is generally accepted that the insulating state results from strong Mott–Hubbard [8] correlation V_{dd} between d-holes on the same cation, which neatly splits the $|d_{x^2-y^2}\rangle$ bands into two bands (completely filled lower Mott–Hubbard band separated by the gap V_{dd} from the upper band). It is also established that all the essential phenomena (superconductivity, magnetism and normal state properties) are confined to the CuO_2 plane; in any subsequent modification brought in due to chemical or stoichiometry change such as introduction of ~15% Sr^{2+} in place of La^{3+}, one introduces 15% holes or excess positive charge in the basal plane and obtains a T_c of ~35 K. In the so-called 123 material ($YBa_2Cu_3O_7$), the mobile hole concentration is ≈3%, with a T_c of ≈90 K. The fundamental question we have to answer is whether the holes introduced result in a Cu^{3+} state (d^2 configuration), in which case, discussion of the deviation from a strictly half-filled Hubbard band (and su-

---

[#] On leave from Groupe des Transitions de Phases, CNRS, Grenoble, France.

[*] To whom all correspondence should be addressed.

0921-4534/88/$03.50 © Elsevier Science Publishers B.V.
(North-Holland Physics Publishing Division)

perconductivity ensuing from it) is relevant, or whether the holes appear elsewhere. This is a question that the spectroscopists have asked themselves and answered. The answer is that all the excess holes introduced end up as holes in the oxygen band (i.e. p^1 state for hole) or O^{1-} with 2p^5 electronic configuration. We therefore have to deal with a partially filled p-band and the physics has little to do with that of almost half-filled Hubbard situation. Let us look at some of the available evidence.

Based on X-ray absorption (Cu K or L edge) spectroscopy, many workers [9–12] initially came to the conclusion that Cu^{3+} was present in $YBa_2Cu_3O_{6.9}$ and $La_{1.85}Sr_{0.15}CuO_4$. Later measurements [13–15] have, however, shown this not to be correct. The 21 eV feature in the Cu K-edge (1s→4p spectrum) earlier attributed to Cu^{3+}, is actually due to the poorly-screened satellite of the 15 eV feature which is its well-screened counterpart. In the absence of Cu^{3+}, the only possibility is that the holes reside on the oxygen orbitals [5,16]. A 1s→2p transition has indeed been identified in the oxygen K-edge spectrum, confirming the presence of holes in the oxygen band [17,18].

We have been investigating the nature of holes in the superconducting cuprates for some time. For this purpose, we have employed photoelectron and Auger electron spectroscopies which provide direct information on the electronic structure [4,5,19]. Since the different valence states of copper would be associated with different binding energies, it becomes possible to determine the nature of the copper species by means of X-ray photoelectron spectroscopy (XPS) and Auger electron spectroscopy. Cu (2p) spectra as well as L_3VV Auger spectra of $La_{1.85}Sr_{0.15}CuO_4$ and $YBa_2Cu_3O_{6.9}$ show the presence of only Cu^{1+} and Cu^{2+} species in the ground state of these oxides, with no detectable amount of Cu^{3+} (figs. 1 and 2). The Cu (2p) spectra show an intense peak due to Cu^{1+} (3d^{10}-final state) at 933 eV and a weaker feature due to Cu^{2+} (3d^9-final state) at 942 eV.

Since these superconducting cuprates contain excess holes due to oxygen-excess stoichiometry, absence of Cu^{3+} would imply that the excess holes reside in the oxygen derived p-band. The O(1s) core level spectra of these cuprates show the presence of features with binding energies of around 529, 531 and 533 eV, respectively (fig. 3). The normally expected oxide species, O^{2-}, with the filled 2p^6 configuration is associated with the 529 eV feature. The O^{1-} species (corresponding to the presence of a hole in the 2p band) is expected to have a slightly higher binding energy than O^{2-}; unfortunately CO_3^{2-} and OH$^-$ which are inevitably present on such oxide surfaces show features around 531 eV. Scraping the sample surface decreases or nearly eliminates the 531 eV feature. We however find an oxygen species with a binding energy of ~533 eV which we consider to be due to the dimerization of O$^-$ holes. While $La_{1.8}Sr_{0.2}CuO_4$ showed only a small contribution due to the dimerized hole species at 300 K in the O(1s) spectrum, the 533 eV signal due to this species is somewhat higher in $YBa_2Cu_3O_{6.9}$. We have studied the O(1s) spectra of a large number of samples of $YBa_2Cu_3O_7$ and all of them inevitably show the ~533 eV feature; non-superconducting $YBa_2Cu_3O_6$, on the

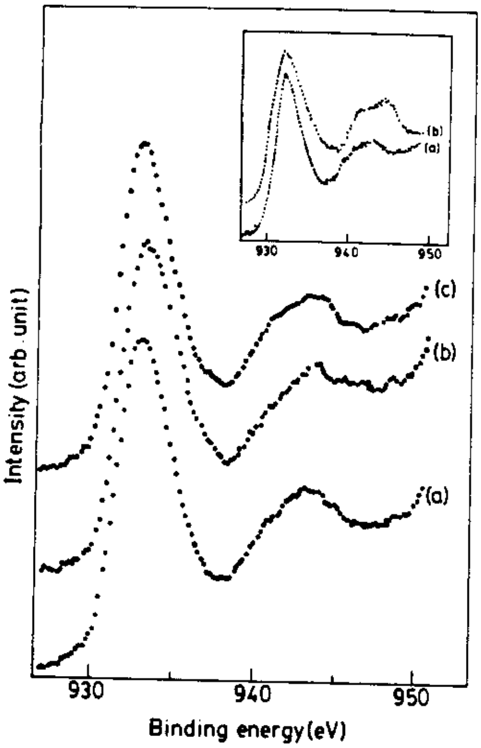

Fig. 1. Cu ($2p_{3/2}$) region in the XPS of $YBa_2Cu_3O_{6.9}$: (a) at 300 K; (b) after cooling to 80 K; (c) after warming the sample (b) back to 300 K. In the inset we show the Cu(2p) spectra of (a) $Tl_2Ca_2Ba_2Cu_3O_{10}$ and (b) $Bi_2(Ca, Sr)_3Cu_2O_8$ at 300 K.

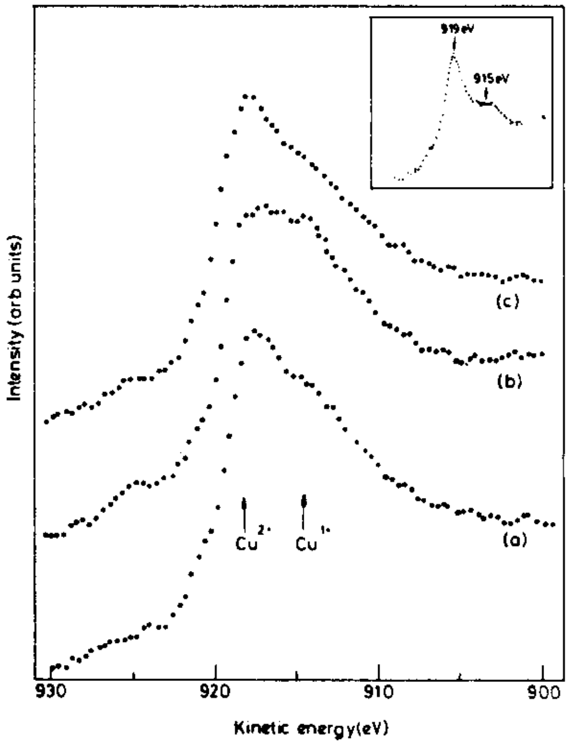

Fig. 2. Cu(L_3VV) Auger spectrum of $YBa_2Cu_3O_{6.9}$: (a) at 300 K; (b) after cooling to 80 K; (c) after warming the sample (b) back to 300 K. In the inset, we show the Cu(L_3VV) spectrum of $Bi_2(Ca,Sr)_3Cu_2O_8$ at 300 K.

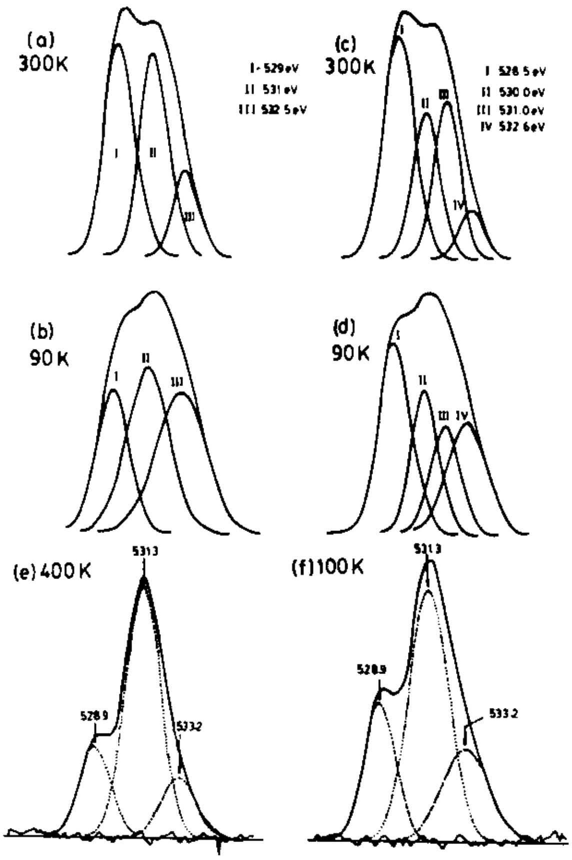

Fig. 3. O(1s) spectra of $YBa_2Cu_3O_{6.9}$ at (a) 300 K and (b) 100 K decomposed into three gaussians; in (c) and (d) we show the O(1s) spectra of unscrapped $Tl_2CaBa_2Cu_2O_8$ at (e) 400 K and (f) 100 K. The ~533 eV feature is seen in all the spectra.

other hand, does not show this feature. Furthermore, our experiments with water have shown that this feature is not due to any species arising from interaction with H_2O. The assignment of the 533 eV O(1s) feature to dimerized oxygen holes O_2^{2-}, is based on the fact that ordinary peroxides and oxygen adsorbed on metal surfaces in the peroxo form show this feature.

The variation of the O(1s) signal intensity due to each species has been studied as a function of temperature in several samples. In fig. 4, we show typical temperature dependence of the 533 eV feature due to the dimerized hole species in the case of $YBa_2Cu_3O_{6.9}$. The proportion of dimerized holes increases substantially with decreasing temperature; the phenomenon is reversible. Accompanying such an increase of the hole dimers with lowering of temperature, the surface conductivity as measured by energy loss spectroscopy [7] increases. We feel that this dimer species plays an important role in the mechanism of superconductivity of these oxides. The preponderant presence of Cu^{1+} in the superconducting state is a noteworthy feature which dictates that a considerable proportion of the oxygens be present in the hole state. The average charge on oxygen would therefore be between one and two while the electron occupation of the d-orbital of Cu would be around 9.5.

Room-temperature Ci(2p) spectra of $Tl_2CaBa_2Cu_2O_8$ ($T_c \sim 110$ K) show a weak feature around 942 eV due to $3d^9$-related final states and an intense feature around 533 eV due to $3d^{10}$-related states (fig. 1). Cu^{1+} appears to be the prominent species in the thallium cuprates as well. Cu(2p) spectra of $Bi_2(CaSr)_3Cu_2O_{8+\delta}$ ($T_c \sim 90$ K) show

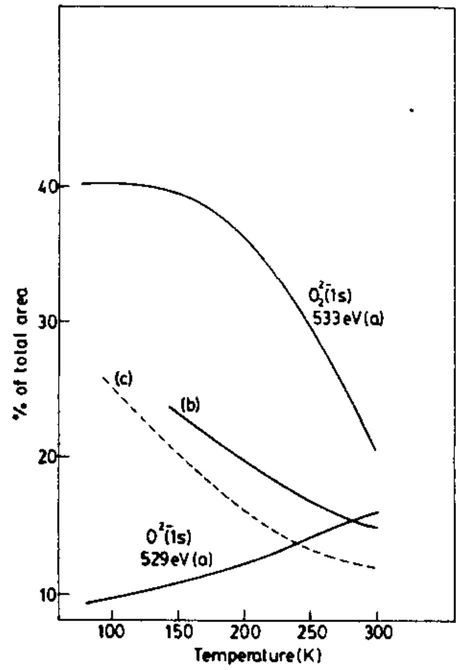

Fig. 4. Temperature variation of the 533 eV feature due to the peroxide-like species in three independent measurements designated (a), (b) and (c). Temperature variation of the 529 eV O^{2-} feature is shown in one case.

similar results (fig. 1); the Cu (LVV) spectrum of this oxide also shows the presence of Cu^{1+} (fig. 2). The proportion of Cu^{1+} seems to increase on lowering the temperature in all these cuprates. It must be noted here that we do not actually expect Cu^{3+} to be present significantly in the Bi and Tl cuprates based on stoichiometry considerations. Furthermore, both Bi and Tl are in the 3+ state in the cuprates as found by X-ray photo emission and chemical means [20]. Presence of Cu^{1+} (and oxygen holes) in the Bi and Tl cuprates therefore assumes considerable significance. The O(1s) spectrum of $Tl_2CaBa_2Cu_2O_8$ reveals that the 533 eV feature due to hole dimers is present even at 400 K and becomes more prominent on cooling (fig. 3), the changes being reversible. (Note the H_2O related species would not be stable above ~240 K.)

3. Pairing states of oxygen holes,

Now that we have established that holes introduced reside on oxygen, it suffices to look at the square plane of 4 oxygens with a copper atom in the middle (fig. 5). The four linear combination of the two p_x (at sites 1 and 3) and two p_y (at sites 2 and 4) are,

$$
\begin{aligned}
|1\rangle &= p_x^1 + p_y^2 + p_x^3 + p_y^4 ,\\
|2\rangle &= p_x^1 - p_y^2 - p_x^3 + p_y^4 ,\\
|3\rangle &= p_x^1 - p_y^2 + p_x^3 - p_y^4 ,\\
|4\rangle &= p_x^1 + p_y^2 - p_x^3 - p_y^4 .
\end{aligned}
\tag{1}
$$

In fig. 5a we show these energy levels; note that only the configuration $|2\rangle$ (of B_{1g} symmetry) will hybridize with the Cu^{2+} $|d_{x^2-y^2}\rangle$ orbital. This is shown in fig. 5b (in a recent publication of Zhang and Rice [21], there seems to be an error in their fig. 1, which actually has zero hybridisation with $|d_{x^2-y^2}\rangle$. Fig. 5c shows, how the oxygen electrons (O^{2-}) spreadout in a filled two-dimensional band. Fig. 6a shows a partially filled O^{2-} band, while fig. 6b depicts it as hole states filled upto the hole Fermi level E_F.

There is the possibility of pairing of the oxygen holes in the k-space, through the intermidiacy of the Cu^{2+} spin, as shown by Emery [22] and Hirsch [23]. Can there also be real-space pairings? With two electrons per orbital of the oxygen band, the ground state

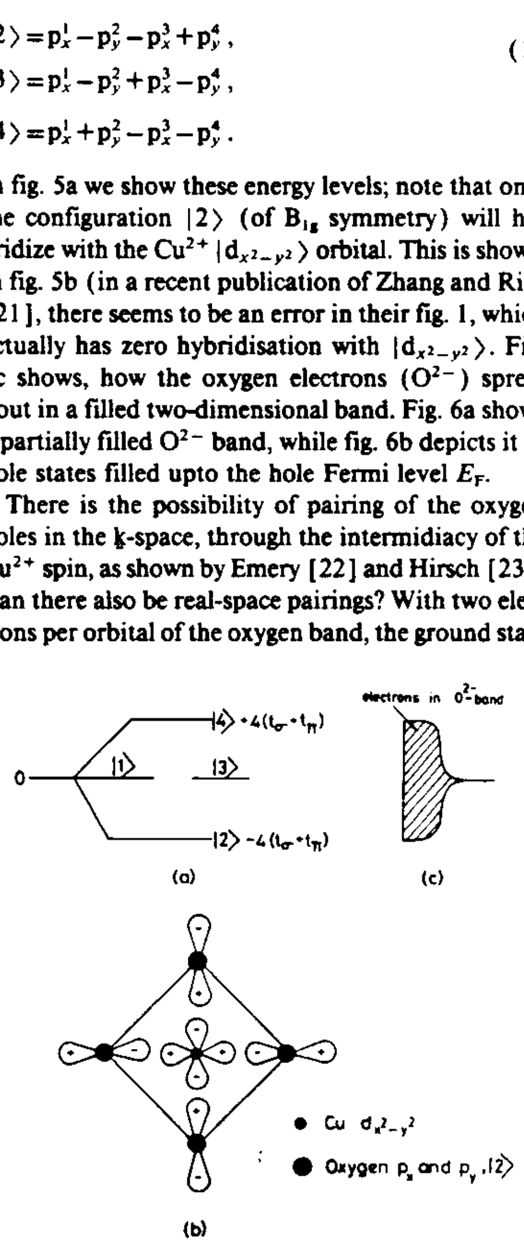

Fig. 5. (a) Energy levels of oxygen orbitals; (b) hybridization of Cu$|d_{x^2-y^2}\rangle$ and oxygen p_x and p_y as in $|2\rangle$; (c) electrons in O^{2-} band.

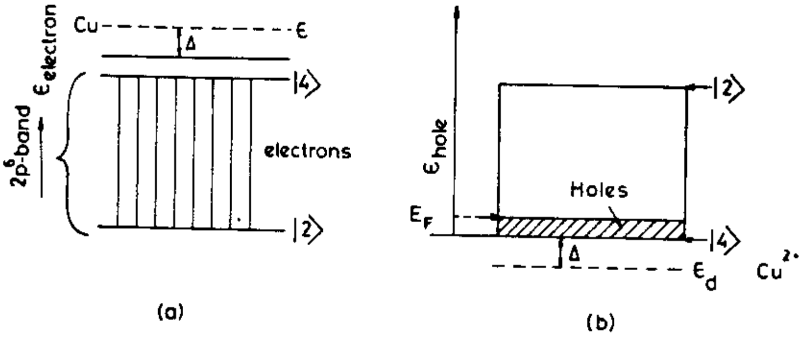

Fig. 6. (a) Electrons in a partially filled O^{2-} band and (b) the corresponding hole picture.

is a filled non-bonding band of electrons unaffected by local lattice deformation. But as soon as holes are added to the top of the electron band (or holes to the bottom of the hole band, fig. 6b), effective bond order is added to the interatomic regions and the lattice responds (see fig. 7) by local bond contraction, which may pull out the empty state below the bottom of the hole band – this is a hole polaron or a hole bipolaron (O^-–O^- dimer). But whether such a bound state will actually occur or not depends critically on the intersite Coulomb repulsion terms between two near neighbour holes, V_{pp} and $V_{pp'}$ depending on whether both are p-holes or one is a $p(O^-)$ the other a d-hole (Cu^{2+}). In fig. 8(a) and (b) we show two possible configurations of (O^-–O^-) hole pairs which we call bipolaron and peroxiton, respectively. If λ is the energy measured from the bottom of the oxygen-hole band, as the coupling energy gained as the pair localises due to deformation, the net binding energy in the two configurations are:

$$E_{\text{bipolaron}} = -\lambda + 4V_{pd} + V_{pp}\,, \tag{2a}$$

$$E_{\text{peroxiton}} = -\lambda + 2V_{pd} + V_{pp} + \Delta\,. \tag{2b}$$

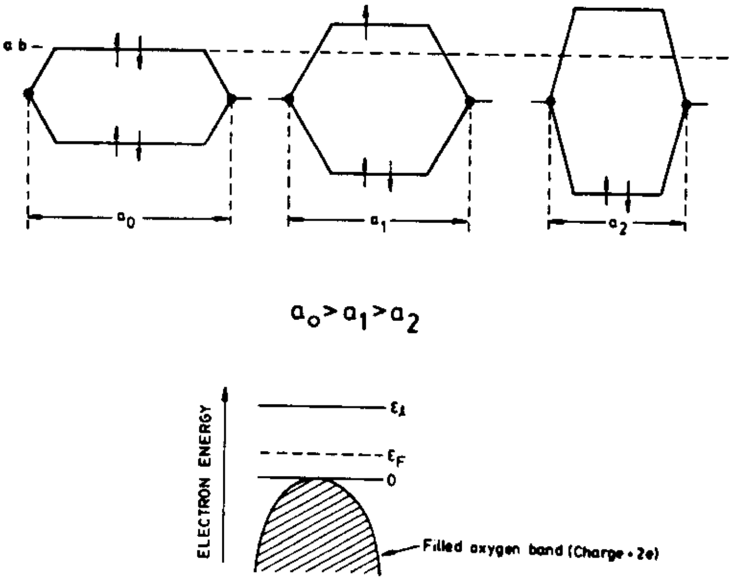

Fig. 7. Bonding and antibonding levels of a filled band are shown on the top part. The inter-atomic distance contracts as electrons are removed from antibonding orbital ($a_2 < a_1 < a_0$). Splitting-off a bound empty (2-hole) state above the antibonding oxygen level is shown at the bottom of the figure.

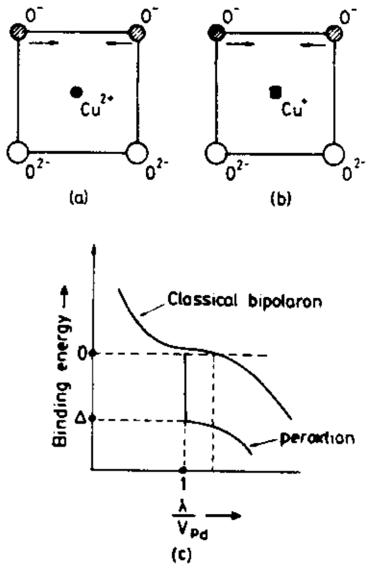

Fig. 8. Configurations of (a) bipolaron and (b) peroxiton; arrows indicate local deformation; (c) binding energies of bipolaron and peroxiton as functions of electron–phonon coupling, λ, and intrinsic Coulomb repulsion, V_{pd}.

Assuming $V_{pp}=0$, to compare (2a) with (2b), we show the position of the binding energies of the bound states in the parameter space (λ/V_{pd}) in fig. 8c. The zero of energy is again the bottom of the oxygen–hole band. Because of the large inter-site Coulomb repulsion ($V_{pd}\sim 1$ eV), the bipolaron would have difficulty in forming a true bound state while the peroxiton (O^-–Cu^+–O^-) pair would have much lower energy. We can also see that the peroxiton binding energy goes abruptly to zero, at some critical value of $\lambda/V_{pp}\sim 1$. At or above such a critical value, peroxiton formation will spontaneously occur, as shown in the energy diagram of fig. 8, where the hole polaron and hole bipolaron levels are also indicated. In a recent publication, Chakraverty et al. [24] have developed the peroxiton hamiltonian in the small p–d hybridisation limit and constructed a new ground state out of 'squeezed phonon vacuum' such that the peroxitons will have an effective mass, $m^*\approx 4$–$10\ m$. These real-space hole pairs can now Bose-Condense at a T_c given by the conventional formlae

$$T_c=\frac{3.31\,\hbar^2}{k_B m^*}\,n_p^{2/3}, \qquad (3)$$

where n_p is the number of peroxitons/cm^3, $\hbar$ the Planck constant and k_B the Boltzmann constant. For $m^*\sim 5$, and $n_p\sim 5\times 10^{21}/\mathrm{cm}^3$, T_c comes out ~ 100 K. Note that the conventional effective mass of a classical bipolaron ~ 100–$1000\ m$ and this gives a $T_c\sim 0$.

4. Discussion

Peroxides are not new to chemistry. Ordinary peroxides such as BaO_2 containing well-defined O–O bonds with a bond order of unity are insulators. The possibility of the existence of peroxide-type species in nominal oxide materials was proposed recently [25] to explain the nature of oxygen excess in $La_2NiO_{4+\delta}$. It was suggested that some of the oxygen in this oxide was present as O_2^{2-} instead of some of the nickel as Ni^{3+}. A study of several oxides where the transition metal is expected to be in a high oxidation state (e.g. $LaCuO_3$, $Ba_2Cu_2O_5$, $Ba_2Ni_2O_5$) has shown the presence of holes in the oxygen 2p band giving rise to O^- species, the metal being present in the normal low-oxidation (2+) state of the transition metal [20]. Superconducting Ba (Pb, Bi)O_3 similarly seems to have Bi^{3+}, Pb^{2+} and oxygen holes. The recent discovery [26] of relatively high T_c (~ 30 K) superconductivity in $Ba_{1-x}K_xBiO_3$ which has no copper is also explained on the basis of oxygen holes (O^-–Bi^{3+}–O^-). While the evidence for the presence of holes in the oxygen 2p bands of oxides may be considered to be of a recent origin, the occurrence of holes in sulphides, selenides and tellurides forming S–S, Se–Se and Te–Te bonds has been known for some time [25,27]. These homopolar species arising from hole dimerization are favoured in the presence of d^{10} ions such as Cu^{1+}. These holes are involved in imparting unusual electrical properties to these chalcogenides. In the light of this information, what we propose here in the case of the superconducting cuprates seems only natural, although energetically we would expect oxygen hole dimers to be less stable than the chalcogen hole dimers (which would follow the order O–O < S–S < Se–Se < Te–Te.

Just as the oxygen holes give rise to superconductivity, they also act to hinder the antiferromagnetic state by progressively killing the superexchange [28] which takes place though filled oxygen ion, O^2. This is shown in (i) and (ii) of fig. 9 for ordinary superexchange which shows that the excited state, by transfer of a spin to a from O^{2-}, can have a favourable admixture of the O^- spin with the cation spin at b, if b is antiparallel to O^-, thus favouring an overall antiferromagnetic ground state of a and b spins. This situation is completely changed if the middle ion is a O^- as shown in the diagram (iii) in fig. 9. Now we see, if the Cu^{2+} ions have parallel spins, both can equally overlap with O^- making the ferromagnetic spin alignment of lower energy. One easily understands why the Mott insulating antiferromagnetic state of the non-superconducting oxides gets easily destroyed as oxygen holes are introduced. Once again, one does not need to invoke any deviation from the half-filled Hubbard band to explain the magnetic results.

In conclusion, we are now in a position to state that the superconductivity and magnetic properties of the high-T_c cuprates can be explained fairly satisfactorily by invoking the presence of peroxitons involving Cu^{1+} and O^- (or paired O^-) species. Takura et al. [29] have recently correlated T_c of cuprates with the [Cu–O] charge in the sheets. We feel that the main $(Cu^z–O^{m-})^p$ species to be considered are, $p=1^+$ with $z=2+$ or $3+$ and $m=1$ or 2 and $p=0$ with $z=1+$ or $2+$ and $m=1$ or 2. The actual charge p is given by the relative proportions of the different species. Since $z=3+$ can be ignored, the superconducting or insulating nature will be determined by the relative proportions of $(Cu^{1+}–O^{1-})$ and $(Cu^{2+}–O^{2-})$.

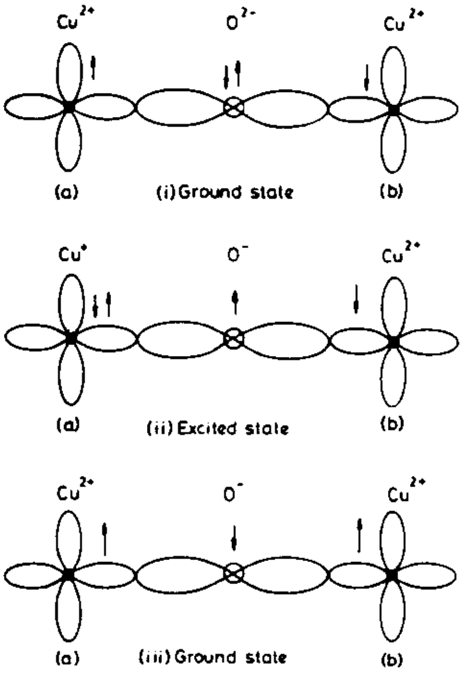

Fig. 9. Interaction of Cu^{2+} and oxygen spins.

Acknowledgement

The authors thank the University Grants Commission and the Department of Science & Technology for support of this research.

References

[1] J.G. Bednorz and K.A. Müller, Z. Phys. B 64 (1986) 189.
[2] P.W. Anderson, Science 235 (1987) 1196.
[3] P.W. Anderson et al., Phys. Rev. Lett. 58 (1987) 2790.
[4] D.D. Sarma, P. Ganguly and C.N.R. Rao, Phys. Rev. B 36 (1987) 2371.
[5] D.D. Sarma and C.N.R. Rao, Solid State Commun. 65 (1988) 47.
[6] A. Bianconi et al., Solid State Commun. 63 (1987) 1009.
[7] D.D. Sarma, K. Prabhakaran and C.N.R. Rao, Solid State Commun. 67 (1988) 263.
[8] N.F. Mott, Metal–Insulator Transitions (Taylor & Francis, London, 1974).
[9] D. Sonderker, D.C. Johnston and W. Eberhardt, Phys. Rev. B 36 (1987) 3983.
[10] G.M. Antonini et al., Euro. Phys. Lett. 4 (1987) 851.
[11] E.E. Alp et al., Phys. Rev. B 35 (1987) 7199.
[12] Y. Jeon et al., Phys. Rev. B 36 (1987) 3891.
[13] P. Steiner et al., Z. Phys. B 67 (1987) 497.
[14] A. Bianconi et al., Int. J. Mod. Phys. 1 (1987) 853.
[15] J.C. Fuggle et al., Phys. Rev. B, Preprint.
[16] A. Fujimori et al., Phys. Rev. B 35 (1987) 8814.
[17] J.A. Yarmoff et al., Phys. Rev. B 36 (1987) 3967.
[18] N. Nucker et al., Z. Phys. B 67 (1987) 9.
[19] C.N.R. Rao et al., Mater. Res. Bull. 22 (1987) 1159.
[20] Unpublished results from this Laboratory.
[21] F.C. Zhang and T.M. Rice, to be published.
[22] V.J. Emery, Phys. Rev. Lett. 58 (1987) 2794.
[23] J.E. Hirsch, Phys. Rev. Lett. 59 (1987) 228.
[24] B.K. Chakraverty et al., Solid State Commun. 64 (1987) 1147.
[25] C.N.R. Rao et al., J. Amer. Chem. Soc. 109 (1987) 6893.
[26] R.J. Cava et al., Nature 332 (1988) 814.
[27] J.C.W. Folmer and F. Jellinek, J. Less Common Metals 76 (1980) 153.
[28] P.W. Anderson, Solid State Physics, Seitz & Turnbull, eds., 14 (1963) 99.
[29] Y. Takura, J.B. Torrance, T.C. Huang and A.I. Nazzal, to be published.

JOURNAL OF SOLID STATE CHEMISTRY 74, 147–162 (1988)

Solid-State Chemistry of High-Temperature Oxide Superconductors: The Experimental Situation*

C. N. R. RAO

Solid State and Structural Chemistry Unit, Indian Institute of Science, Bangalore 560012, India

Received November 10, 1987; in revised form December 2, 1987

High-temperature superconductivity in oxides of the type (La, $Ln)_{2-x}Ba_x(Sr)_xCuO_4$, $Y(Ln)Ba_2Cu_3O_{7-\delta}$, $La_{3-x}Ba_{3+x}Cu_6O_{14}$, and related systems is discussed with emphasis on aspects related to experimental solid-state chemistry. All of these oxides possess perovskite-related structures. Oxygen-excess and La-deficient La_2CuO_4 also exhibit superconductivity in the 20–40 K just as $La_{2-x}Ba_x(Sr_x)CuO_4$; these oxides are orthorhombic in the superconductivity phase. The crucial role of oxygen stoichiometry in the superconductivity of $YBa_2Cu_3O_{7-\delta}$ ($T_c = 95 \pm 5$ K) is examined; this oxide remains orthorhombic up to $\delta \approx 0.6$ and becomes tetragonal and nonsuperconducting beyond this value of δ. Oxygen stoichiometry in this and related oxides has to be understood in terms of structure and disorder. The structure of $La_{3-x}Ba_{3+x}Cu_6O_{14}$ is related to that of $YBa_2Cu_3O_7$, the orthorhombic structure manifesting itself when the population of O1 oxygens (along the Cu–O–Cu chains) is preponderant compared to that of O5 oxygens (along the *a*-axis); nearly equal populations of O1 and O5 sites give rise to the tetragonal structure. A transition from a high-T_c (95 K) superconductivity regime to a low-T_c (~60 K) regime occurs in $YBa_2Cu_3O_{7-\delta}$ accompanying a change in δ. There is no evidence for Cu^{3+} in these nominally mixed valent copper oxides. Instead, holes are present on oxygens giving rise to O^- or O_2^{2-} species, the concentration of these species increasing with the lowering of temperature. Certain interesting aspects of the superconducting oxides such as domain or twin boundaries, Raman spectra, microwave absorption, and anomalous high-temperature resistivity drops are presented along with the important material parameters. Preparative aspects of the superconducting oxides are briefly discussed. Phase transitions seem to occur at T_c as well as at ~240 K in $YBa_2Cu_3O_7$.

1. Introduction

The phenomenon of superconductivity has been an area of vital interest for the past few decades. Metals, alloys, molecular compounds, and polymers have been investigated for superconductivity, but the transition temperature did not cross the 23 K threshold until the beginning of 1987. The average rate of increase in T_c was about 3 K per decade. The highest T_c's in the 20 K region were exhibited by A15 compounds such as Nb_3Ge. Some of the more interesting chemical systems examined were Chevrel phases, organic donor–acceptor systems, and charge-transfer salts. Among the metal oxides, the highest T_c's were found in $LiTi_2O_4$ (*1*) and $BaPb_{1-x}Bi_xO_3$ (*2*), both close to 13 K. The possibility of high-temperature superconductivity in metal oxides was first demonstrated by Bednorz and

---

[*] Contribution No. 494 from the Solid State and Structural Chemistry Unit.

0022-4596/88 $3.00

Müller (*3*) in the La–Ba–Cu–O system. It was soon found that these oxides had the general formula $La_{2-x}Ba_xCuO_4$ and possessed the quasi-two-dimensional K_2NiF_4 structure; the analogous Sr compounds also showed high T_c superconductivity, the maximum T_c (20–40 K) in the Sr and Ba systems being at $x = 0.2$ and 0.15, respectively (*4–6*). Soon after this discovery, superconductivity above liquid nitrogen temperature was reported in the Y–Ba–Cu–O system (*7*); the phase responsible for superconductivity in this system was found to have the composition $YBa_2Cu_3O_{7-\delta}$ with a defect perovskite structure (*8, 9*).

The discovery of superconductivity above the liquid nitrogen temperature in metal oxides has raised much hope because of obvious technological implications. Of equal importance is the fact that this has given a big boost to research in the solid-state chemistry of metal oxides. The unprecedented excitement caused by the discovery of high T_c oxide superconductors as well as the flood of research publications and conference proceedings on the subject appearing in the last few months have prompted me to write this brief overview article, to highlight the major experimental findings (up to November 1987) of relevance to solid-state chemistry. In writing such an article, it was necessary to exercise the difficult discipline of quoting only representative references which would permit the reader to obtain the necessary details. If I have ignored some important references, I apologize for any errors in judgment.

2. La_2CuO_4 and Its Derivatives

Oxides of the general formula A_2BO_4 possess the K_2NiF_4 structure wherein the *B* ions interact only in the *ab* plane. The structure and properties of oxides of the K_2NiF_4 structure have been examined in some detail recently (*10*). La_2CuO_4 which is a member of this family, exhibits low resistivity (~1 ohm · cm) at room temperature, but the resistivity increases with decreasing temperatures, with a tendency to become antiferromagnetic. Electrical and magnetic properties of La_2CuO_4 are very sensitive to oxygen stoichiometry. Antiferromagnetism in La_2CuO_4 has been recently established by neutron diffraction and scattering; T_N is close to 290 K with a low-temperature Cu moment of 0.43 μ_B (*11*). The oxide undergoes an orthorhombic-tetragonal distortion at 505 K. It has been suggested that La_2CuO_4 is in a two-dimensional quantum fluid state wherein the spins are ordered instantaneously over long distances, but no measurable time-averaged moment has been detected (*11*). More interestingly, oxygen-excess La_2CuO_4 prepared under high oxygen pressure or by plasma oxidation becomes superconducting near 40 K (*12, 13*); lanthanum deficiency (e.g., $La_{1.9}CuO_4$) gives rise to superconductivity even with ordinary ceramic preparations (*14*) as shown in Fig. 1. It is to be noted that both oxygen-excess and La-deficiency give rise to a nominal mixed valency of Cu as in $La_{2-x}Ba_xCuO_4$.

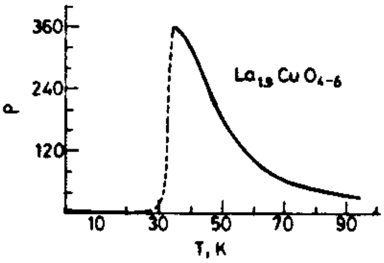

FIG. 1. Superconducting transition in La-deficient La_2CuO_4 [from Ref. (*14*)].

When La in orthorhombic La_2CuO_4 is partly replaced by Sr or Ba, the structure becomes tetragonal at room temperature, for $x > 0.05$ in $La_{2-x}Ba_x(Sr_x)CuO_4$. These oxides exhibit superconductivity in the 20–40 K range (*4–6*), the T_c peaking near $x =$ 0.15 and 0.2 (nom.) for Ba and Sr, respectively. A Meissner effect up to 70% of the

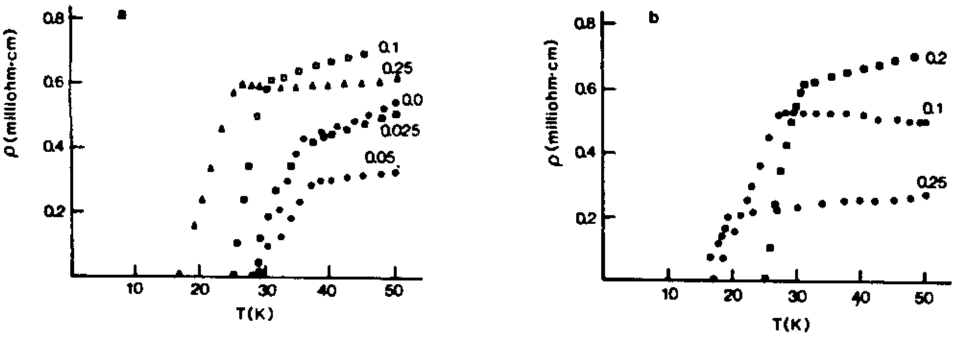

FIG. 2. (a) Resistivity data of $(La_{1-y}Pr_y)_{1.8}Sr_{0.2}CuO_4$ for different values of y. (b) Resistivity data of $(La_{0.9}Pr_{0.1})_{2-x}Sr_xCuO_4$ for different values of x [Ref. (*15*)].

ideal value has been reported in these oxides. $La_{2-x}Ca_xCuO_4$ also exhibits superconductivity, but the T_c values are much lower (*15, 16*); for example, the maximum value of T_c is 20 K for $x = 0.1$ (compared to 26 K when $x = 0.2$ Sr). The room-temperature structure of $La_{1.85}Sr_{0.15}CuO_4$ involves copper atoms with a tetragonally elongated octahedral coordination and Cu–O distances of 1.898 and 2.406 Å; La and Sr sites have ninefold oxygen coordination (*17*). Superconductivity is found in the 15–30 K region in oxides of the type $(La_{1-y}Ln_y)_{2-x}Ba_x(Sr_x)CuO_4$ where Ln = Pr, Nd, Eu, Gd, etc. (*15, 16, 18*) as shown in Fig. 2. In all such systems, T_c reaches a maximum at a particular value of x suggesting the importance of strong correlations (*19*).

$La_{2-x}Ba_x(Sr_x)CuO_4$ undergoes a tetragonal-orthorhombic distortion near 180 K, the orthorhombic distortion increasing smoothly (through T_c) down to 30 K (*20*). Static and dynamic aspects of the tetragonal-orthorhombic distortion in $La_{2-x}Sr_xCuO_4$ have been studied by neuron scattering and other techniques and a classical soft phonon behavior involving CuO_6 octahedra has been observed (*21*). ESR studies have thrown light on the microscopic magnetic interactions in these oxides (*22*).

The replacement of Cu in $La_{2-x}Ba_x(Sr_x)CuO_4$ by Ni even to a small extent lowers the T_c and superconductivity is destroyed at ~5% substitution; Zn substitution has a similar effect although the ionic sizes of Zn^{2+} and Ni^{2+} differ from that of Cu^{2+} in the opposite directions (*13, 15*).

It is noteworthy that electrical resistivity values of $La_{2-x}Ba_x(Sr_x)CuO_4$ in the normal state are generally in the 10^{-2}–10^{-3} ohm · cm range which correspond to Mott's minimum metallic conductivity (*18*). These oxides are typical type II superconductors with H_{c1} = 400 Oe (4.7 K); H_{c2} is in the range 40–70 T (*23*). Far infrared measurements show the superconducting gap to be ~50 cm^{-1} (*24*). The magnetic penetration depth in $La_{1.85}Ba_{0.15}CuO_4$ is reported to be ~2000 Å (*25*).

3. $YBa_2Cu_3O_{7-\delta}$ and Related Oxides

Superconductivity above liquid N_2 temperature was reported in $Y_{1.2}Ba_{0.8}CuO_4$ by Wu *et al.* (*7*) who prepared this composition by analogy with the $La_{2-x}Ba_xCuO_4$ system, expecting that the smaller Y ion would increase T_c due to chemical pressure effects. This composition was actually biphasic consisting of green (insulating) Y_2BaCuO_5 and a black oxide. Since Y_2CuO_4 itself is not known to crystallize in the K_2NiF_4 structure, Rao and co-workers (*9*) examined the Y–Ba–Cu–O system starting with compositions of the type $Y_{3-x}Ba_{3+x}Cu_6O_{14-\delta}$, by analogy with the defect perovskite $La_{3-x}Ba_{3+x}Cu_6O_{14-\delta}$ described by

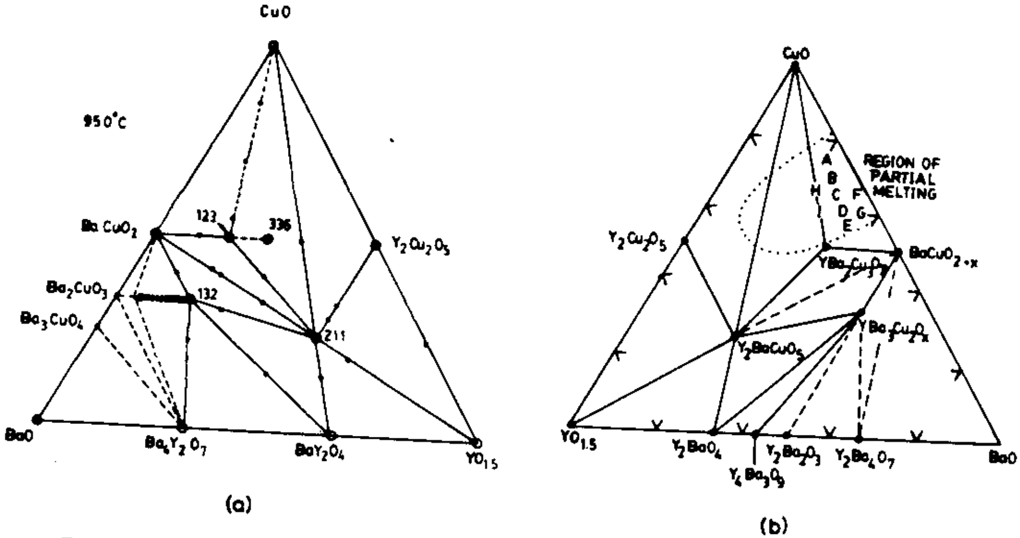

FIG. 3. (a) Pseudo-ternary phase diagram of the Y_2O_3–BaO–CuO system at 1220 K slightly modified from that published by Clarke (*75*). Here, 123, 211, and 132 refer to $YBa_2Cu_3O_{7-\delta}$, Y_2BaCuO_5, and $YBa_3Cu_2O_x$, respectively. The dashed line joining CuO to the superconducting phase (123) is a joint at 1170 K but is interrupted by melting 1200 K. The hatched line shows a region of apparent solid solution and the dotted lines emanating from it reflect uncertainty in end-member composition. We have shown the 336 oxide $Y_3Ba_3Cu_6O_{14}$ or the $Y(Ba_{2-x}Y_x)Cu_3O_7$ system although this system is likely to be stable around 1120 K or lower. (b) Phase diagram of the same system at 1240 K from Roth *et al.* (*76*).

Er-Rakho *et al.* (*26*). The perovskite phase responsible for high T_c (95 ± 5 K) superconductivity in the Y–Ba–Cu–O system is orthorhombic $YBa_2Cu_3O_{7-\delta}$ (*8, 9*); the highest Meissner effect found hitherto in this oxide is ~80%. The phase diagram of the Y_2O_3–BaO–CuO system has been investigated by several workers [see, for example, Ref. (*27*)], and among the many phases, only $YBa_2Cu_3O_{7-\delta}$ has been clearly established to be a high-T_c superconductor (Fig. 3). $Y_{3-x}Ba_{3+x}Cu_6O_{14-\delta}$ with $x = 0.0$–0.5 also seems to be superconducting, although the phasic purity of these compositions is not fully established.

Superconductivity in $YBa_2Cu_3O_{7-\delta}$ is extremely sensitive to oxygen stoichiometry. Samples where the oxygen content is higher than 7 have also been made and they show $T_c \approx 90$ K up to 7.2 (*28*). When $\delta \geq 0.6$, the oxide becomes tetragonal and nonsuperconducting; oxygen is readily intercalated into the oxygen-deficient samples until the stoichiometry becomes close to $YBa_2Cu_3O_7$. In Fig. 4, the variation of the unit cell parameters of $YBa_2Cu_3O_{7-\delta}$ with δ is shown; notice how the structure becomes tetragonal at $\delta \approx 0.6$. The unit cell volume increases with δ from ~173.7 Å^3 ($\delta = 0.0$) to ~176.2 Å^3 ($\delta = 1.0$).

The structure of orthorhombic $YBa_2Cu_3O_{7-\delta}$ is interesting. It has corner-linked CuO_4 planar groups connected not only as sheets in the *ab* plane, but also as chains parallel to the *b*-axis (*29, 30*) as shown in Fig. 5(a). Of the two sets of Cu atoms, one is surrounded by four oxygens at 1.929 and 1.960 Å; a fifth oxygen is located at 2.30 Å, giving rise to a square-pyramidal coordination for Cu, forming puckered CuO_2 sheets. In the other set, the Cu atoms are surrounded by four oxygens at 1.942 Å and 1.845 Å; here, the oxygen atoms form near rectangles connected by vertices, and resulting in the chains along the b-axis. These chains are responsible for the orthorhombic structure. In the tetragonal $YBa_2Cu_3O_6$ (δ = 1.0), the chains are missing as shown in Fig. 5(b) and the oxygens occupy only two-thirds of the perovskite anion sites and are ordered in such a manner that one-third of the Cu atoms is twofold coordinated while two-thirds is fivefold coordinated (*31*, *32*); the Cu–O4 bond in this oxide is indeed very short (~1.80 Å). In Fig. 5(c), we also show a tetragonal phase where oxygen disorder (δ = 0.3–1.0) can give rise to distorted CuO_6 octahedra (*33*). Oxygen nonstoichiometry in $YBa_2Cu_3O_{7-\delta}$ has to be understood in terms of both disorder and structural distortion. If the O1 sites (oxygen along the chains) are predominently populated relative to the O5 sites (along a-axis) the structure is orthorhombic and the material is a superconductor. If the O1 and O5

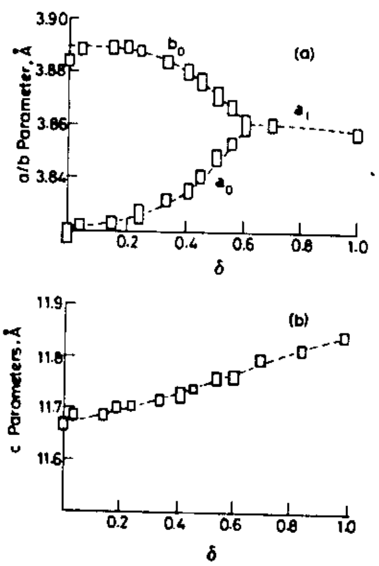

FIG. 4. Variation of the unit cell parameters of $YBa_2Cu_3O_{7-\delta}$ with δ. Notice that the orthorhombic a_0 and b_0 parameters merge to give the tetragonal a_t parameters around δ = 0.6.

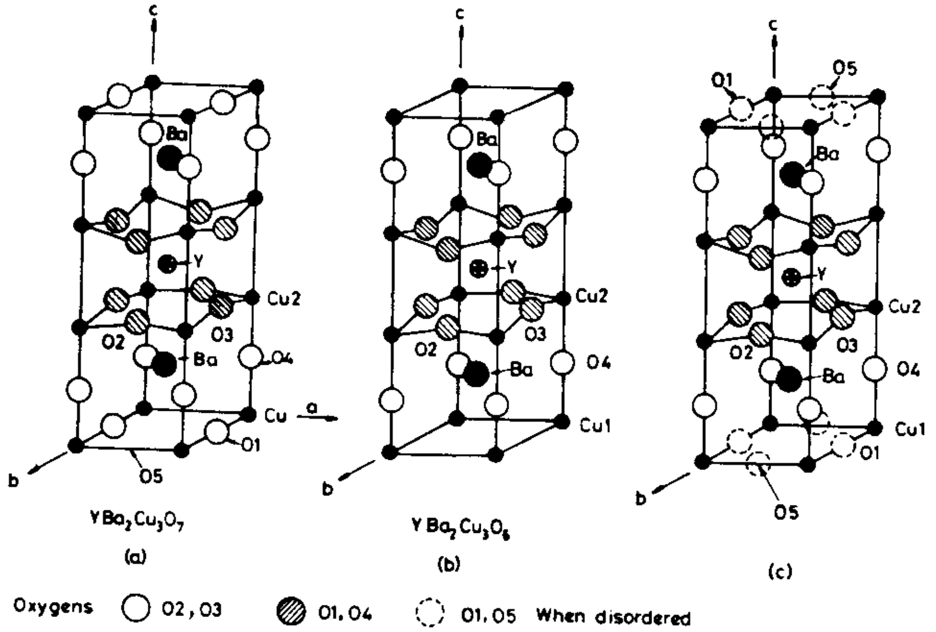

FIG. 5. Structures of $YBa_2Cu_3O_{7-\delta}$: (a) orthorhombic structure of the superconducting phase with δ = 0.0; (b) tetragonal structure of the nonsuperconducting phase with δ = 1.0; (c) disordered structure of the tetragonal phase involving CuO_6 octahedra with a small site occupancy. If the chain oxygen (O1) sites are predominantly occupied relative to oxygens along the a-axis (O5 sites), the structure will be orthorhombic; equal population of O1 and O5 sites makes it tetragonal. The Cu–O4 distance varies with stoichiometry. In (a) the O1–O4 distance is quite short (~2.6 Å).

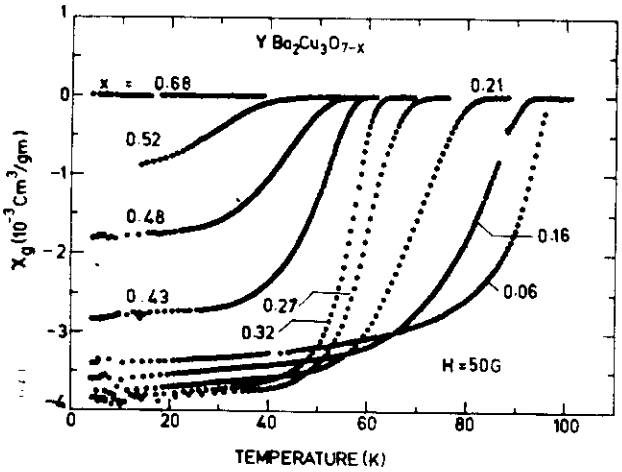

FIG. 6. Meissner effect (at 50 G) of $YBa_2Cu_3O_{7-\delta}$ for different values of δ [from Ref. (*39*)].

sites are equally populated, the structure is tetragonal. Ordering of oxygens in the chains seems crucial for high-T_c superconductivity. A slight off-site displacement of the O1 (possibly of O5) oxygens also must be considered. Quenching $YBa_2Cu_3O_7$ from high temperature results in oxygen loss and the associated orthorhombic-tetragonal transition occurs in the 620–700 K range, depending on the oxygen pressure, around $\delta \approx 0.5$ (*33*).

Superconducting oxides of the general formula $LnBa_2Cu_3O_7$ with Ln = Nd, Sm, Eu, Gd, Dy, Ho, Er, Tm, Yb, Lu have all been prepared; they are all orthorhombic similar to $YBa_2Cu_3O_7$ with $T_c \approx 90$ K (*34–37*). Magnetic states seem to coexist along with superconductivity in the oxides containing paramagnetic lanthanides such as Gd (*38*). Oxides of this general composition with the variable valence elements Ce, Pr, and Tb are not superconducting and their structures seems to be different. $LaBa_2Cu_3O_{7-\delta}$ (orthorhombic) also contains Cu–O–Cu chains and is superconducting; the T_c, however, varies widely (40–90 K) depending on the preparative conditions. Observation of high-T_c superconductivity in a number of lanthanide compounds analogous to $YBa_2Cu_3O_7$ indicates that the Y/Ln ion does not have a major role to play in the superconductivity except to hold the structure together. At T_c, there appears to be an isostructural phase transition, at least in $YBa_2Cu_3O_7$, as revealed by specific heat, nuclear quadrupole resonance, thermal expansion, and other measurements.

The variation of the superconducting transition temperature of orthohombic $YBa_2Cu_3O_{7-\delta}$ with δ(0.0–0.6) is most interesting. In Fig. 6, the magnetic susceptibility data of $YBa_2Cu_3O_{7-\delta}$ for different values of δ (*39*) are shown. In Fig. 7, resistivity data (*40*) of different compositions are presented. We have plotted the T_c values from resistivity and susceptibility data against δ in Fig. 8. While T_c remains nearly constant near 90 K when δ = 0.0–0.2 it drops to a lower value (~60 K) above δ = 0.2 showing a plateau-like behavior. Since in this plateau region, the Cu–O–Cu chains of $YBa_2Cu_3O_7$ are deficient in oxygen, it is possible that the ~60 K plateau is more characteristic of the CuO_2 sheets in the orthorhombic structure, the 90 K T_c being more characteristic of the Cu–O–Cu chains in the presence of the CuO_2 sheets (the sheets getting coupled through the chains). Figure 8 may

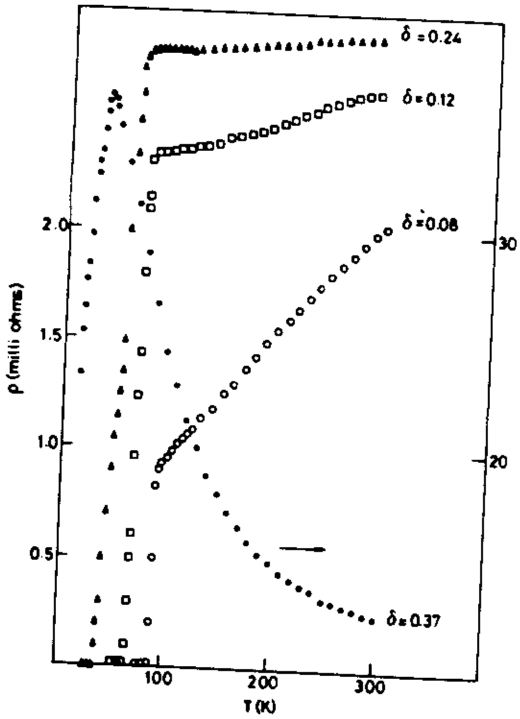

FIG. 7. Electrical resistivity behavior of $YBa_2Cu_3O_{7-\delta}$ for different values of δ [from Ref. (*40*)].

be taken to signify a transition from chain-type superconductivity to sheet-type superconductivity in $YBa_2Cu_3O_{7-\delta}$, brought about by a change in oxygen stoichiometry. Accordingly, the Hall coefficient and the volume fraction subject to the Meissner effect are also insensitive in the plateau region; Although the actual T_c values at different δ vary slightly among different workers (*41*), there is little doubt regarding the presence of the constant low-T_c plateau at $\sim 0.2 \leq \delta \leq 0.5$. Whether there is a unique structural feature in the plateau region is not yet certain, although certain superlattice spots in diffraction patterns (or diffuse scattering) seem to have been noticed in this composition range. Electrical resistivity and magnetic susceptibility reflect the unique nature of the compositions in the plateau region.

Several workers have in recent months synthesized a variety of derivatives of $YBa_2Cu_3O_{7-\delta}$. The Y/Ba or *Ln*/Ba ratio in Y(*Ln*)$Ba_2Cu_3O_7$ has been varied (*37, 42*), with a slight alteration of T_c. Ba has been partly replaced by La causing a decrease in the lability of oxygen. Substitution of Ba by Sr or *Ln* in $YBa_2Cu_3O_{7-\delta}$ lowers the T_c (*43*). Cu in $YBa_2Cu_3O_{7-\delta}$ has been partly substituted by Zn, Ni, Co, Fe, and other ions, and such substitutions generally lower T_c or destroy the superconductivity, the structure tending to be tetragonal or/and oxygen-deficient (see, for example, Refs. (*13, 44*)). Weakly orthorhombic or nearly tetragonal samples prepared by low-temperature methods exhibit low T_c or no superconductivity. Oxygen-deficient $YBa_2Cu_3O_{7-\delta}$ (δ up to 0.7) have been prepared in the orthorhombic structure by the low-temperature Zr-getter technique; these samples show superconductivity with T_c exhibiting a plateau in the $\delta = 0.3$–0.45 region (*45*); T_c, however, decreases markedly when $\delta > 0.45$. The question then arises as to whether the orthorhombic structure (with Cu–O–Cu chains) is necessary to achieve a high T_c. There are some unconfirmed reports of tetragonal analogs of $YBa_2Cu_3O_7$ exhibiting

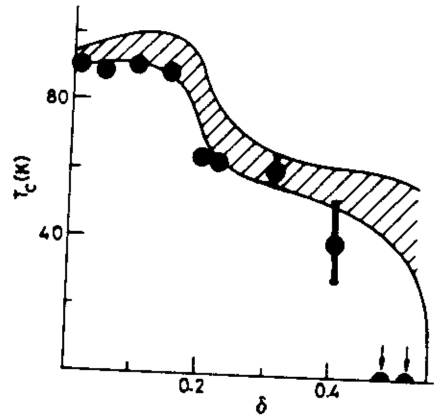

FIG. 8. Variation of T_c with δ. Magnetic measurements of Johnston *et al.* [Ref. (*39*)] are indicated by the cross-hatched region. Our resistivity data is shown by full dark circles.

high T_c in the 80–90 K range (e.g., $YBa_2Cu_{3-x}Ga_xO_7$); structures of such oxides however need to be confirmed by neutron studies, since X-ray diffraction alone would not be able to establish unequivocally the tetragonality of the structure. Another possibility is that the tetragonal structure arises from a randomness of Cu–O chains (along *a*- and *b*-axes) or that it is due to the absence of long-range order with respect to the Cu–O chains.

Samples of $YBa_2Cu_3O_{7-\delta}$ which show high-T_c superconductivity exhibit fairly high resistivity (Mott's minimum metallic conductivity range) in the normal state (*18*). The absolute thermopower and Hall effect measurements of the samples with $\delta < 0.5$ show that oxides of these compositions are *p*-type (hole) conductors. The electronic properties of $YBa_2Cu_3O_{7-\delta}$ [as well as of $La_{2-x}Ba_x(Sr_x)CuO_4$] are anisotropic. A "superconducting glass-type" behavior has been noticed in these oxides by Müller and others based on magnetic measurements.

Some of the important properties of this type II superconductor are summarized below (*46*):

Hall carrier density: 4×10^{21} cm^{-3} (for a material of resistivity ~ 400 $\mu\Omega$ cm just above the T_c).

$dH_{c2}/dT = 2T/K$; BCS coherence length ≈ 1.4 nm; London penetration depth ≈ 200 nm; mean free path ≈ 1.2 nm.

$H_c(O) \approx 1T$.

$H_{c2}(O) \approx 120T$.

Critical current density: In ceramic samples, $\sim 10^3$ A/cm^2 at 77 K; in films (on $SrTiO_3$) $\sim 10^5$ A/cm^2 at 77 K; at 4.2 K, $\sim 10^6$ A/cm^2 (in crystals and films).

Depairing current density: 10^7–10^8 A/cm^2 (estimated).

A critical current density of $\sim 10^5$ A/cm^2 is essential for viable magnet and other applications at 77 K. A magnetic penetration depth of 225 ± 75 Å has been recently reported as an upper limit for $YBa_2Cu_3O_7$ (*25*). Recent specific heat (*c*) measurements on $YBa_2Cu_3O_7$ show $\Delta c/T_c$ to be ~ 48 mJ/mol · K^2 giving rise to a $\Delta c/\gamma T_c$ of 1.33; there is a large temperature dependence of the Debye temperature, probably due to the large vibrational amplitudes of the loosely bound O1 and O2 oxygens in the orthorhombic structure (*47*). It is interesting to consider whether this feature has a bearing on the tendency to form peroxide species (see Section 4). It is to be noted that the O1–O4 distance is rather short (Fig. 5a).

Oriented thin films of superconducting $YBa_2Cu_3O_{7-\delta}$ have been prepared by employing electron beam or pulsed laser evaporation (*48*). The substrate used is generally $SrTiO_3$. Since these films show sharp transitions and high critical currents, their potential in electronic applications seems promising.

Raman and infrared spectra of $YBa_2Cu_3O_{7-\delta}$ and related oxides have been examined by several workers (*49–51*). There has however been considerable disagreement in the assignments. Many workers report Raman bands close to 340, 440, 500, 580, and 630 cm^{-1}, of which the last is somewhat of a mystery peak with variable intensity from sample to sample. The 630-cm^{-1} band has not been reported by some workers; the band is also not found in $YBa_2Cu_3O_6$. The 630-cm^{-1} Raman band has been assigned to the Raman-inactive Cu–O chain stretching mode and also to "defect clusters," but this band could also arise from the O–O stretching mode of a peroxide-like species or due to an impurity such as $Y_2Cu_2O_5$. The 580-cm^{-1} band shows an increase in intensity with increasing δ, while the 500-cm^{-1} band shows evidence of softening. The 500-cm^{-1} band is most likely due to the Cu–O stretching mode involving the short Cu–O bonds along the *c*-axis. The 370- to 330-cm^{-1} bands are due to Cu–O deformation modes. There is some uncertainty regarding the assignment of the 430- and 580-cm^{-1} Raman bands which have been attributed to

Cu–O stretching in the sheets. The infrared spectrum of $YBa_2Cu_3O_7$ shows only a few bands instead of the expected 21. We are able to assign an infrared band around 580 cm^{-1} to a mode involving the Cu–O (chain) stretching in $YBa_2Cu_3O_7$ and a band close to 600 cm^{-1} in $YBa_2Cu_3O_6$ due to Cu–O stretching involving the short Cu–O bonds (along the *c*-axis or possibly the disordered CuO_6 octahedra in the tetragonal structure). In $YBa_2Cu_3O_7$ an IR band close to 190 cm^{-1} (associated with Y) and another at 140 cm^{-1} (associated with Ba or with a Cu–O chain bend) are seen clearly, just as in the Raman studies. Far infrared studies have been reported to show a superconducting gap starting at 210 cm^{-1} (*49*), but there seems to be some uncertainty about this observation.

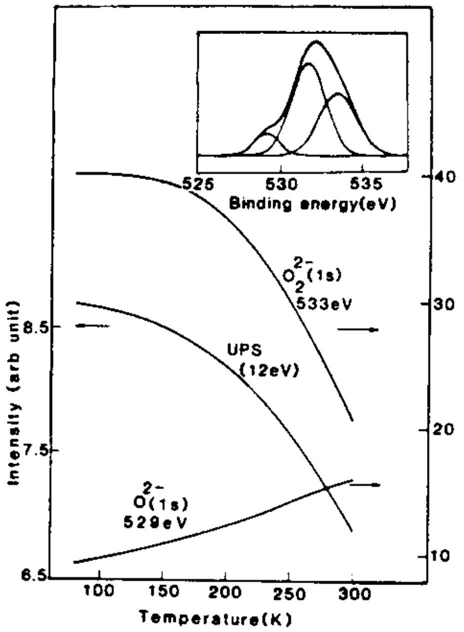

FIG. 9. Temperature-variation of O(1s) peak intensity due to O^{2-} and O_2^{2-} species (at 529 and 533 eV, respectively) in $YBa_2Cu_3O_7$. Temperature-variation of the intensity of He II spectrum at 12 eV is also shown. Inset shows the O(1*s*) signal at 80 K as consisting of three Gaussians peaking at 529, 531, and 533 eV; the one at 531 eV is due to O^- species [from Ref. (*52*)].

4. Nature of the Cu Species and the Role of Oxygen

We have seen earlier how oxygen plays a crucial role in the superconductivity of $YBa_2Cu_3O_{7-\delta}$. Careful studies by employing photoelectron and Auger spectroscopies have thrown much light on this aspect. Ultraviolet photoemission spectroscopy studies show some changes in the 12-eV region in the case of $YBa_2Cu_3O_7$ on cooling the sample to 80 K. The valence band region clearly shows a low density of states at the Fermi level and indicates the presence of strong correlations. Variable-temperature X-ray photoelectron spectroscopy studies on $La_{1.8}Sr_{0.2}CuO_4$ and $YBa_2Cu_3O_7$ in the O(1s) and Cu(2p) regions (*52, 53*) indicate the presence of molecular oxygen species with a high O(1s) binding energy of ~533 eV alongside of features due to the oxide and O^- or/and impurity) ions around 529 and 531 eV, respectively (Fig. 9). The proportion of species responsible for the 533-eV feature increases with the lowering of temperature (Fig. 9). This oxygen species is identified as a peroxide-like unit (although it is close to the feature expected for ice) based on the knowledge of O(1*s*) binding energies of such species generated by oxygen adsorbed on transition metal surfaces as well as of traditional metal peroxides. The Cu(2*p*) spectrum shows the presence of a well-screened d^{10} state (Cu^{1+}) at 933 eV, along with a poorly screened d^9 state (Cu^{2+}) at 942 eV. The proportion of the d^{10} state increases with the lowering of temperature. There is, however, no evidence for Cu^{3+} in the Cu(2*p*) or Auger spectra; X-ray absorption edge measurements also provide no evidence for Cu^{3+} (*54*). Auger spectra, however, clearly show the presence of Cu^{1+} (Fig. 10).

Based on the above findings, it has been proposed that holes are present on oxygen rather than on copper in $YBa_2Cu_3O_7$ and

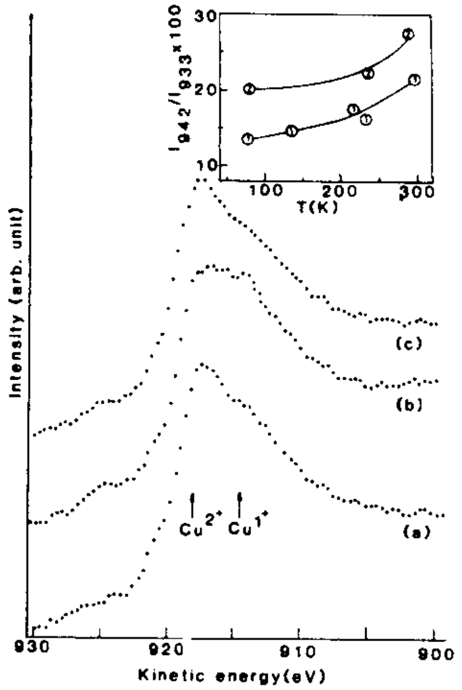

FIG. 10. Cu(L_3VV) Auger spectrum of $YBa_2Cu_3O_7$ at different temperatures. In the inset, the temperature variation of the intensity of the 942-eV feature relative to that of the 933-eV feature in the Cu($2p_{3/2}$) spectrum is shown. The circled numbers 1 and 2 refer to independent sets of measurements (results from this laboratory). (a), (b) and (c) are at 300, 80 and 300 K respectively.

$La_{2-x}Ba_x(Sr_x)CuO_4$ (note that both are hole conductors). The oxygen holes (O^-) could then dimerize to give peroxide-type species (O_2^{2-}). The pair of electrons released in the formation of such species from the oxide ions ($2O^{2-} \rightarrow 2O^-$ or $O_2^{2-} + 2e$) could be related to superconductivity. It is likely that the average charge on oxygen in these oxides is close to $-1.3 + 0.1$. Holes in the O($2p$) valence bands are favored by the Cu^{1+} (d^{10}) state, just as holes in the S($3p$) or Se($4p$) valence bands are generally favored in the Cu^{1+} chalcogenides (*52*). Since there is no real evidence for Cu^{3+} and the Cu–O bonds are highly covalent (1.8–1.95 Å), we conclude that the contribution from the state with the holes on Cu is indeed negligible. It may be noted here that peroxide-like species are likely to be common in many oxides which are supposed to contain metal ions in high-oxidation states (e.g., Pb^{4+}, Ni^{3+}, Cu^{3+}).

5. $La_{3-x}Ba_{3+x}Cu_6O_{14}$ and Related Oxides

High-T_c superconductivity up to 70 K in the $La_{3-x}Ba_{3+x}Cu_6O_{14+\delta}$ (the so-called 336) system (*55*, *56*) created considerable interest since the structure was then known to be tetragonal (*26*) with no Cu–O–Cu chains in evidence. Oxygen treatment under pressure increases T_c; Sr substitution for Ba is also possible. Recent neutron diffraction studies (*57*) of a few members of this family have shown that these oxides are in fact disordered isomorphs of orthorhombic $YBa_2Cu_3O_{7-\delta}$ and that they do contain Cu–O–Cu chains. (A tetragonal structure has, however, been assigned to these materials by some workers, based on X-ray studies.) In these oxides, both the O1 and O5 sites are partially occupied, with more oxygen atoms in the O1 site. Equal occupation of the O1 and O5 sites would give rise to the tetragonal structure. If one takes the normalized difference in the O1 and O5 site occupancies as an order parameter, the zero-resistance T_c increases with the order parameter. The nonsuperconducting $x = 0$ compound corresponding to $La_3Ba_3Cu_6O_{14+\delta}$ itself has the tetragonal $YBa_2Cu_3O_{7-\delta}$ structure with partial substitution of La on the Ba sites (*58*). The $x = 1$ compound, $LaBa_2Cu_3O_{7-\delta}$, is orthorhombic, with a reported T_c as high as 90 K (*59*); a T_c of ~77 K is more commonly found in this laboratory. As mentioned earlier, T_c in this compound depends very markedly on the stoichiometry and ordering of oxygens especially in the chain (more so that in $YBa_2Cu_3O_{7-\delta}$), just as in the other members of the $La_{3-x}Ba_{3+x}Cu_6O_{14+\delta}$ family. We find $La_{3-x}Ba_{3+x}Cu_6O_{14+\delta}$ to be tetragonal with oxygen excess and low T_c.

The observation that the structure of $La_{3-x}Ba_{3+x}Cu_6O_{14-\delta}$ is related to that of $YBa_2Cu_3O_{7-\delta}$ (possessing Cu–O–Cu chains) is important. This relationship clearly justifies the very early characterization of $YBa_2Cu_3O_{7-\delta}$ (*9, 60*) on the basis of the structure of $La_{3-x}Ba_{3+x}Cu_6O_{14}$. This also makes it worthwhile to investigate the $Y_{3-x}Ba_{3+x}Cu_6O_{14}$ system (*9, 60*) carefully. By employing low-temperature methods, it has been possible to synthesize monophasic $Y_{3-x}Ba_{3+x}Cu_6O_{14}$ as well as $(Y, La)_{3-x}Ba_{3+x}Cu_6O_{14}$. These aspects as well as the synthesis of the $Ln_{3-x}Ba_{3+x}Cu_6O_{14}$ family of oxides are being examined in detail in this laboratory. It now appears as though all the oxides showing high-T_c superconductivity are orthorhombic. Where one apparently encounters tetragonality, it would be necessary to establish the structure unequivocally by neutron diffraction.

6. Some Novel Features

Nominal mixed valence, low-dimensionality, and marginal metallicity in the normal state are three of the important features of these oxide superconductors. Electronic and magnetic properties are anisotropic as expected of low-dimensional materials. While $La_{2-x}Sr_xCuO_4$ seems to exhibit measurable ^{18}O isotope effect on the T_c, there is essentially no isotope effect in the case of $YBa_2Cu_3O_{7-\delta}$ (*61*). There is some news that marginal isotope effect has been found in some laboratories. While we cannot entirely ignore electron–phonon interaction, its direct role as in the traditional BCS theory is not apparent. It is possible that if the relevant phonon mode softens in the temperature region of interest the isotope effect will be masked (K. P. Sinha, unpublished results). Excitonic bands around 0.5 and 1.0 eV seem to be present in $La_{2-x}Sr_xCuO_4$ and the significance of these bands needs to be further explored.

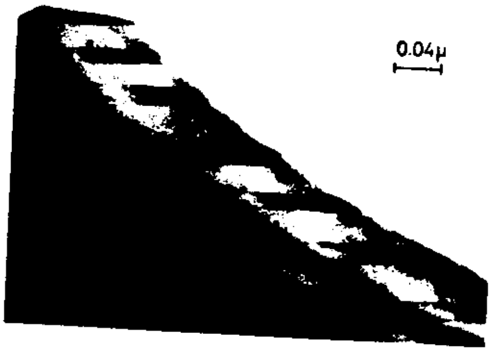

FIG. 11. Bands in electron micrographs of $YBa_2Cu_3O_7$ due to twins [from Ref. (*62*)].

Electron microscopic studies of $YBa_2Cu_3O_7$ show the presence of domain or twin boundaries (Fig. 11), in addition to other defects (*40, 42, 62–64*). It is important to understand the nature of such domains, since the coherence length is only a few angstroms. Twins such as those in Fig. 11 can arise from the different orientations of the $(CuO_2)_\infty$ units in the orthorhombic structure; along the boundaries, there could be oxygen excess compared to the bulk (*40, 64*). The possibility that the microstructural features arise from the separation of metallic and insulating phases in these borderline metals has to be considered. Control of the microstructure (twin density) provides a means of optimizing the critical density (*65*). It is to be noted that twins arise from the orthorhombic structure which in turn becomes possible due to the presence of Cu–O–Cu chains. Properties such as grain size (boundaries) and sample porosity are also crucial material parameters.

Many samples of $YBa_2Cu_3O_{7-\delta}$ and related oxides are reported to exhibit sharp resitivity anomalies at relatively high temperatures (200–300 K). Inverse AC Josephson effect has also been employed to examine this behavior (*66*). Such observations are generally irreproducible in the sense that these properties do not persist over repeated cycles or on standing for ex-

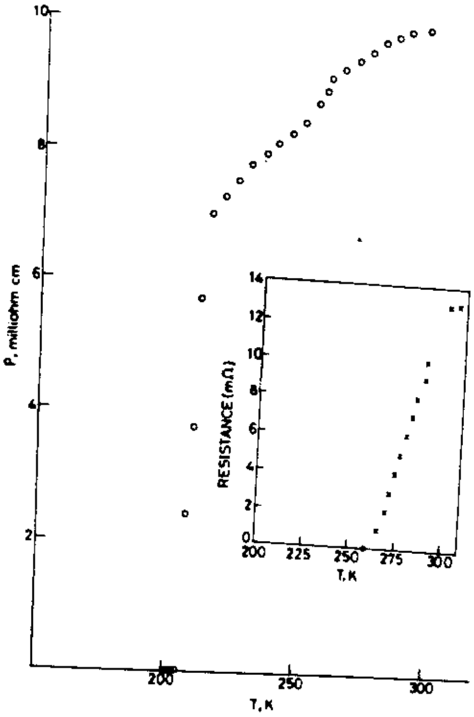

FIG. 12. A sample of $Y_2Ba_2Cu_3O_x$ where Ba sites are partly substituted by La prepared in the author's laboratory showing zero-resistance around 210 K. Inset shows a similar behavior seen in $ErBa_2Cu_3O_{7-\delta}$ by Ayyub *et al.* (77).

tended periods. It seems that many of these observations are artifacts of the electrical measurement techniques or of sample inhomogeneity, especially in samples prepared at high temperatures (27). "Zero-resistance" has also been occassionally observed at 200 K or above by some workers in certain oxide compositions; adequate Meissner effect measurements on such samples are lacking. In Fig. 12, we show such a transition found in this laboratory, but unfortunately this feature disappeared on recycling giving back the 95 K transition. It should be noted here that the volume fraction of the 95 K superconducting phase in $YBa_2Cu_3O_7$ itself is rather small (~15%). The phase responsible for T_c values of 200 K or higher may therefore be present only in small proportions. It is possible that intergrowths are responsible for such a behavior, but it is not clear why they should be unstable. The challenge is to obtain a stable, pure sample of such a really hot oxide superconductor, if it exists.

In the superconducting state, $YBa_2Cu_3O_7$ absorbs electromagnetic radiation over a wide range of frequencies from a few megahertz to a few gigahertz (*67*). The intensity of absorption is very sensitive to temperature, particle size, and magnetic field, and crucially depends on the presence of ambient oxygen. Josephson junctions formed by oxygen and the superconducting grains may be responsible for this effect.

A large increase in T_c (up to 160 K) has been found by cycling across 239 K (*71*) and this may be considered to be due to oxygen ordering or movement. It is equally possible that the microstructure (twin density) changes across this transition. A 234 K transition has been encountered, based on a temperature-variation study of the 640-cm^{-1} Raman band (*72*); this transition correlates with acoustic anomalies and may represent a continuous transition involving change in point group symmetry (D_{2h}–C_{2v}). The 234–239 K transition needs to be investigated in detail by acoustic and other measurements since such a transition (also found in $La_{2-x}Ba_xCuO_4$) may be fundamental to superconductivity in these oxides.

7. Preparative and Related Aspects

The synthesis of superconducting oxides provides many opportunities and challenges. The most common method employed is the ceramic method involving the high-temperature reaction of an appropriate mixture of oxides and carbonates. Citrates and oxalates have also been employed with no definitive advantage in the case of $La_{2-x}Ba_x(Sr_x)CuO_4$ and $YBa_2Cu_3O_7$; nitrates, however, seem to have a definitive advantage (*68*). In the synthesis of $YBa_2Cu_3O_7$ and related oxides, we have found it convenient to employ BaO_2 instead of $BaCO_3$.

Starting with a slight excess of CuO sharpens the transition. Addition of BaF_2 seems to have a similar effect. The effect of partial fluorination is yet to be carefully investigated, although there are indications that T_c increases significantly, in this process.

The precursor method (*69*) would be an ideal alternative route for the synthesis of these oxides. Unfortunately, no single precursor compound or a precursor solid solution has been found. Mixed nitrates, however, seem to be useful *in* preparing oxide superconductors which specially require low temperatures [e.g., $Y_{3-x}(La_{3-x})Ba_{3+x}Cu_6O_{14}$]. Precipitation from high alkaline media has not been successful. The sol–gel route in the traditional sense seems difficult because it is hard to get the alkoxides of Y(*Ln*), Ba, and Cu^{2+} to form a homogeneous mix. It may be worthwhile to examine the feasibility of using cuprous alkoxides (instead of cupric) for the sol–gel route. It has been possible to prepare gels by adding appropriate amounts of yttrium nitrate and copper acetate to a known amount of barium hydroxide (*13*). Oxides of the La–Ba–Cu–O system can similarly be prepared starting with lanthanum nitrate.

Heating under high oxygen pressure is found convenient for producing stoichiometric or oxygen-excess samples. Thus, superconducting $La_2CuO_{4+\delta}$ and $La_{3-x}Ba_{3+x}Cu_6O_{14-\delta}$ have been made by treatment under high oxygen pressure. Plasma oxidation offers another convenient way of preparing such materials. $La_2CuO_{4+\delta}$ has been prepared by plasma oxidation; $YBa_2Cu_3O_{7-\delta}$ ($\delta \approx 0.5$–1.0) is readily oxidized to the near-stoichiometric phase by plasma oxidation (*13*). Different workers have prepared $YBa_2Cu_3O_{7-\delta}$ by employing different treatments. The time of annealing (soaking) in oxygen varies quite markedly, from a few hours to a few days. In general, most preparations yield samples with T_c in the 90–95 K region. Some workers have reported much higher T_c values (>100 K) in samples annealed or soaked differently (*70*); for example, soaking samples of $YBa_2Cu_3O_7$ for extended periods in a helium or a nitrogen atmosphere has been reported to increase T_c up to 130 K, but the effect does not appear to be permanent. These results are generally based on electrical resistivity measurements. The chemistry of such treatments is not clear. One possibility is that oxygen in the Cu–O–Cu chains becomes perfectly ordered, causing an increase in T_c; it is worthwhile to examine the Meissner effect in such samples.

Exposure of $YBa_2Cu_3O_7$ and other oxide superconductors to laboratory atmosphere for extended periods seems to degrade the materials. In the case of $YBa_2Cu_3O_7$, hydroxides and carbonates of the component metals and surface carbonization have been noticed especially when samples are impure.

Samples of $YBa_2Cu_3O_7$ and other oxides prepared by low-temperature methods generally exhibit low T_c values. Part of the problem could be the small particle size which in turn determines the nature of grain boundaries. Single crystals of $La_{2-x}Ba_x(Sr_x)CuO_4$ and $YBa_2Cu_3O_{7-\delta}$ have been grown by the flux method by several workers. In particular, the recent work by Holtzberg *et al.* (*73*) on the growth of $YBa_2Cu_3O_{7-\delta}$ crystals is noteworthy.

8. Concluding Remarks

The tremendous possibilities of applications of $YBa_2Cu_3O_7$ and other yet-to-be-discovered high-T_c ceramic oxides make this area of research most exciting. Clearly, the high-temperature oxide superconductors constitute the most sensational discovery since the transistor. There is considerable scope for obtaining reliable data on these oxide superconductors. Theories and models will have to wait until the experimental findings are fully established and the future offers unlimited scope for research in metal oxide solid-state chemistry. Superconductivity near room temperature or above is often being reported, but no stable phase of this type has yet been isolated. It is possible that a stable room-temperature superconductor is lying somewhere in a solid-state chemistry laboratory. Many oxide systems, especially those containing V, Nb, and Ru, as well as intergrowth structures (*74*) such as (Y, Ba, $Sr)_{n+1}Cu_nO_{3n+1}$, need to be investigated. What is especially satisfying is that even in this short period, there is an appreciation of the role of structure and stoichiometry in superconductivity. Thus, Cu–O–Cu chains are responsible for the orthorhombic structure of $YBa_2Cu_3O_7$, and the orthorhombic structure is essential for the formation of twins which control many of the properties. Furthermore, all the high-T_c oxides discussed hitherto belong to the perovskite family and possess orthorhombic structures.

Acknowledgments

The author is thankful to the U.S. National Science Foundation, University Grants Commission, and the Department of Science and Technology for support.

Note added in proof. Linearity of normal-state resistivity of $YBa_2Cu_3O_7$ over a wide temperature range is noteworthy. Hitherto, there is no clear evidence for vacancy ordering in $YBa_2Cu_3O_{7-\delta}$, especially when $\delta = 0.33$ or 0.5. Incorporation of an extra Cu–O layer is supposed to increase T_c to 290 K (*78*), but we have not been able to confirm this observation. The 240 K transition in $YBa_2Cu_3O_7$ is confirmed by heat capacity measurements (*79*).

$Ln_{3-x}Ba_{3+x}Cu_6O_{14+\delta}$ (Ln = La, Nd, etc.) becomes tetragonal at a value of x depending on Ln; these members have low T_c compared to the 123 system. In the La member, only the $x = 1.0$, $\delta \approx 0.0$ shows high T_c (*80*).

Two-dimensional $Sr_2Bi_2Cu_2O_{7+\delta}$ is superconducting (*81*).

References

1. D. C. Johnston, H. Prakash, W. H. Zachariasen, and R. Viswanathan, *Mater. Res. Bull.* **8,** 777 (1973).

2. A. W. Sleight, J. L. Gillson, and F. E. Bierstedt, *Solid State Commun.* **17,** 27 (1975).

3. J. G. Bednorz and K. A. Müller, *Z. Phys. B* **64,** 187 (1986).

4. R. J. Cava, R. B. van Dover, B. Batlogg, and E. A. Reitman, *Phys. Rev. Lett.* **58,** 408 (1987).

5. C. W. Chu, P. H. Hor, R. L. Meng, L. Gao, Z. J. Huang, and Y. Q. Wang, *Phys. Rev. Lett.* **58,** 405 (1987).

6. S. Uchida, H. Takagi, K. Kitazawa, and S. Tanaka, *Japan. J. Appl. Phys.* **26,** L1 (1987).

7. M. K. Wu, J. R. Ashburgn, C. J. Torng, P. H. Hor, R. L. Meng, L. L. Gao, Z. J. Huang, Y. Q. Wang, and C. W. Chu, *Phys. Rev. Lett.* **58,** 908 (1987); Z. Zhao *et al. Kexue Tongbao,* No. 6 (1987).

8. T. Siegrist, S. Sunshine, D. W. Murphy, R. J. Cava, and S. M. Zahurak, *Phys. Rev. B* **35,** 7137 (1987); R. J. Cava, B. Batlogg, R. B. van Dover, D. W. Murphy, S. Sunshine, T. Siegrist, J. P. Remeika, E. A. Rietman, S. Zahurak, and G. P. Espinosa, *Phys. Rev. Lett.* **58,** 1676 (1987).

9. C. N. R. Rao, P. Ganguly, A. K. Raychaudhuri, R. A. Mohan Ram, and K. Sreedhar, *Nature (London)* **326,** 856 (1987).

10. P. Ganguly and C. N. R. Rao, *J. Solid State Chem.* **53,** 193 (1984).

11. S. Mitsuda, G. Shirane, S. K. Sinha, D. C. Johnston, M. S. Alvarez, D. Vaknin, and D. E. Moncton, *Phys. Rev. B* **36,** 822 (1987); G. Shirane, Y. Endoh, R. J. Birgeneau, M. A. Katsner, Y. Hidaka, M. Oda, M. Suzuki, and T. Murakami, *Phys. Rev. Lett.* **59,** 1613 (1987).

12. J. Beille, R. Cabanel, C. Chaillout, B. Chevalier, G. Demazeau, F. Deslandes, J. Etorneau, P. Le Jay, C. Michel, J. Provost, B. Raveau, A. Sulpice, J. Tholence, and R. Tournier, *C. R. Acad. Sci. Paris* **18,** 304 (1987).

13. J. M. Tarascon, P. Bardoux, B. G. Bagley, L. H. Greene, W. R. McKinnon, and G. W. Hull, *ACS Symp. Ser.* **351,** Chap. 20 (1987).

14. S. M. Fine, M. Greenblatt, S. Simizu, and S. A. Friedberg, *ACS Symp. Ser.* **351,** Chap. 10 (1987).

15. P. Ganguly, R. A. Mohan Ram, K. Sreedhar, and C. N. R. Rao, *Solid State Commun.* **62,** 807 (1987); R. A. Mohan Ram, P. Ganguly, and C. N. R. Rao, *Phase Transitions* **10,** 107 (1987).

16. A. K. Grover, S. K. Dhar, P. L. Paulose, V. Nagarajan, E. V. Sampath Kumaran and R. Nagarajan, *Solid State Comm.* **63,** 1003 (1987).

17. H. H. Wang, U. Geiser, R. J. Thorn, K. D. Carlson, M. A. Beno, M. R. Monaghan, T. J. Allen, R. B. Proksch, D. L. Stupka, W. K. Kwok, G. W. Crabtree, and J. M. Williams, *Inorg. Chem.* **26,** 1190, 1474 (1987).

18. C. N. R. Rao, *Int. J. Mod. Phys. B* **1,** 721 (1987).

19. K. Sreedhar, T. V. Ramakrishnan, and C. N. R. Rao, *Solid State Commun.* **63,** 835 (1987).

20. P. Day, M. Resseinsky, K. Prassides, W. I. F. David, O. Moze, and A. Soper, *J. Phys. C. Solid State* **20,** L429 (1987).

21. R. J. Birgeneau, C. Y. Chen, D. R. Grabbe, H. P. Jenssen, M. A. Kastner, C. J. Peters, P. J. Picone, T. Thio, T. R. Thurston, and H. L. Tuller, to be published.

22. H. Thomann, D. C. Johnston, P. J. Tindall, D. P. Goshorn, and R. A. Klemm, *Phys. Rev. Lett*, in press.

23. K. Nakao, N. Miura, S. Uchida, H. Takagi, S. Tanaka, K. Kishio, J. Shimoyama, K. Kitazawa, and K. Fueki, *Japan. J. Appl. Phys.* **26** (1987); D. W. Capone, D. G. Hinks, J. D. Jorgensen, and K. Zhang, to be published.

24. Z. Schlesinger, R. L. Greene, J. D. Bednorz, and K. A. Muller, *Phys. Rev. B* **35,** 7232 (1987).

25. R. Felici, J. Penfold, R. C. Ward, E. Olsi, and C. Matacotta, "RAL-87-062," Rutherford Appleton Laboratory Report (1987); *Nature* (*London*) **329,** 523 (1987).

26. L. Er-Rakho, C. Michel, J. Provost, and B. Raveau, *J. Solid State Chem.* **37,** 151 (1981).

27. J. B. Torrance, E. M. Engler, V. Y. Lee, A. I. Nazzal, Y. Tokura, M. L. Ramirez, J. E. Vazquez, R. D. Jacowitz, and P. M. Grant, *ACS Symp. Ser.* **351,** Chap. 9 (1987).

28. S. W. Keller, K. J. Leary, T. A. Faltens, J. N. Michaels, and A. M. Stacey, *ACS Symp. Ser.* **351,** Chap. 12 (1987).

29. W. I. F. David, W. T. A. Harrison, J. M. F. Gunn, O. Moze, A. K. Soper, P. Day, J. D. Jorgensen, M. A. Beno, D. W. Capone, D. G. Hinks, I. K. Schuller, L. Soderholm, C. U. Segre, K. Zhang, and J. D. Grace, *Nature* (*London*) 327, 310 (1987).

30. F. Beech, S. Miraglia, A. Santoro, and R. S. Roth, *Phys. Rev. B* **35,** 8778 (1987).

31. P. Bordet, C. Chaillout, J. J. Capponi, J. Chenavas, and M. Marezio, *Nature* (*London*) **327,** 687 (1987).

32. A. Santoro, S. Miraglia, F. Beech, S. A. Sunshine, D. W. Murphy, L. F. Schneemeyer, and J. V. Waszczak, *Mater. Res. Bull.* **22,** 1009 (1987).

33. J. D. Jorgensen, M. A. Beno, D. G. Hinks, L. Soderholm, K. J. Volin, R. L. Hitterman, J. D. Grace, I. K. Schuller, C. U. Segre, K. Zhang, and M. S. Kleefisch, *Phys. Rev. B* **35,** 7915 (1987).

34. R. A. Mohan Ram, N. Y. Vasantacharya, and C. N. R. Rao, *J. Solid State Chem.* **69,** 186 (1987); J. M. Tarascon, W. R. McKinnon, L. H. Greene, G. W. Hull, and E. M. Vogel, *Phys. Rev. B* **36,** 226 (1987).

35. D. W. Murphy, S. A. Sunshine, R. B. van Dover, R. J. Cava, B. Batlogg, S. M. Zahurak, and L. F. Schneemeyer, *Phys. Rev. Lett.* **58,** 1888 (1987).

36. K. N. Yang, Y. Dalichaouch, J. M. Ferriera, B. W. Lee, J. J. Neumeier, M. S. Torikachvili, H. Zhou, M. B. Maple, and R. R. Hake, *Solid State Commun.* (1987).

37. C. C. Torardi, E. M. McCarron, M. A. Subramanian, H. S. Horowitz, J. B. Michel, A. W. Sleight, and D. E. Cox, *ACS Symp. Ser.* **351,** Chap. 15 (1987).

38. B. D. Dunlap, M. Slaski, D. G. Hinks, L. Soderholm, M. Beno, K. Zhang, C. Segre, G. W. Grabtree, W. K. Kwok, S. K. Malik, I. K. Schuller, J. D. Jorgensen, and Z. Sungaila, *J. Magn. Magn. Mater.* **68,** 139 (1987); G. V. Subbarao, U. V. Varadaraju, R. Vijayashree, K. Padmanabhan, R. Balakrishnan, T. A. Mary, N. P. Raju, R. Srinivasan, U. De, J. Janaki, and T. S. Radhakrishnan, *Proc. Yamada Conf. Low-Temp.* (1987).

39. D. C. Johnston, A. J. Jacobson, J. M. Newsam, J. T. Lewandowski, D. P. Goshorn, D. Xie, and W. B. Yelon, *ACS Symp. Ser.* **351,** Chap. 14 (1987).

40. C. N. R. Rao, L. Ganapathi, and R. A. Mohan Ram, *Mater. Res. Bull*, in press.

41. Z. Z. Wang, J. Calyhold, N. Pong, J. M. Tarascon, L. H. Greene, W. R. McKinnon, and G. W. Hull, *Phys. Rev. B* **36,** 7222 (1987); R. J. Cava, B. Batlogg, C. H. Chen, E. A. Rietman, S. M. Zahurak, and D. Werder, *Nature* (*London*) **329,** 423 (1987).

42. C. N. R. Rao, P. Ganguly, K. Sreedhar, R. A. Mohan Ram, and P. R. Sarode, *Mater. Res. Bull.* **22,** 849 (1987).

43. K. Fueki, K. Kitazawa, K. Kishio, T. Hasegawa, S. Uchida, H. Takagi, and S. Tanaka, *ACS Symp. Ser.* **351,** Chapter 4 (1987).

44. J. Thiel, S. N. Song, J. B. Ketterson, and K. R. Poeppelmeier, *ACS Symp. Ser.* **351,** Chap. 17 (1987); Y. Maeno *et al.*, *Nature* (*London*) **328,** 512 (1987).

45. R. J. Cava, B. Batlogg, C. H. Chen, E. A. Rietman, S. M. Zahurak, and D. Werder, *Nature* (*London*) **329,** 423 (1987).

46. A. P. Malozemoff, W. J. Gallagher, and R. E. Schwall, *ACS Symp. Ser.* **351,** Chap. 27 (1987).

47. K. Kadowaki *et al.* to be published.

48. P. Chaudhari, R. H. Koch, R. B. Laibowitz, T. R. McGuire, and R. J. Gambino, *Phys. Rev. Lett.* **55,** 2684 (1987); X. D. Wu, D. Dijkkamp, S. B. Ogale, A. Inam, E. W. Chase, P. F. Miceli, C. C. Chang, J. M. Tarascon, and T. Venkatesan, *Appl. Phys. Lett.* **51,** 861 (1987).

49. M. Cardona, L. Genzel, R. Liu, A. Wittlin, H. Mattausch, F. Garcia-Alvarado, and F.

Garua-Gonzalez, *Solid State Commun.* **64**, 727 (1987).

50. Z. Iqbal, S. W. Steinhauser, A. Bose, N. Cipollini, and H. Eckardt, *Phys. Rev. B* **36**, 2283 (1987); G. A. Kourouklis, A. Jayaraman, B. Batlogg, R. J. Cava, M. Stavola, D. M. Krol, E. A. Rietman, and L. F. Schneem Eyer, to be published.
51. Y. Dai, J. S. Swinnea, H. Steinfink, J. B. Goodenough, and A. Campion, *J. Amer. Chem. Soc.* **109**, 5291 (1987).
52. C. N. R. Rao, P. Ganguly, M. S. Hegde, and D. D. Sarma, *J. Amer. Chem. Soc.* **109**, 6983 (1987); C. N. R. Rao, P. Ganguly, J. Gopalakrishnan, and D. D. Sarma, *Mater. Res. Bull.* **22**, 1159 (1987).
53. D. D. Sarma and C. N. R. Rao, *J. Phys. C.* **20**, L659 (1987); D. D. Sarma, K. Sreedhar, P. Ganguly, and C. N. R. Rao, *Phys. Rev. B* **36**, 2371 (1987).
54. P. Steiner, V. Kinsinger, I. Sander, B. Siegwart, S. Hüfner, C. Politis, R. Hoppe, and H. P. Müller, *Z. Phys. B* **67**, 497 (1987); A. Bianconi, A. Clozza, A. C. Castellano, S. D. Longa, M. De Santis, P. Delongu, A. Gargano, R. Giorgi, P. Lagarde, A. M. Flank, and A. Maceili, *Int. J. Mod. Phys.* **1**, 853 (1987).
55. D. B. Mitzi, A. F. Marshall, J. Z. Sun, D. J. Webb, M. R. Beasley, T. H. Geballe, and A. Kapitulnik, to be published.
56. A. K. Ganguli, L. Ganapathi, K. Sreedhar, R. A. Mohan Ram, P. Ganguly, and C. N. R. Rao, *Pramana* **29**, 335 (1987).
57. C. U. Segre, B. Dabrowski, D. G. Hinks, K. Zhang, J. D. Jorgensen, M. A. Beno, and I. K. Schuller, *Nature (London)* **329**, 227 (1987).
58. W. I. F. David, W. T. A. Harrison, R. M. Ibberson, M. T. Weller, J. R. Grasmeder, and P. Lanchester, *Nature (London)* **328**, 328 (1987).
59. A. Maeda *et al.*, *Japan. J. Appl. Phys.* **26**, L1366 (1987).
60. R. A. Mohan Ram, K. Sreedhar, A. K. Ray Chaudhuri, P. Ganguly, and C. N. R. Rao, *Philos. Mag. Lett.* **55**, 257 (1987); P. Ganguly, K. Sreedhar, A. K. Raychaudhuri, and C. N. R. Rao, *Pramana* **27**, 229 (1987).
61. B. Batlogg, R. J. Cava, J. Jayaraman, R. B. Van Dover, G. A. Kourokis, S. Sunshine, D. W. Murphy, L. W. Rupp, H. S. Chen, A. White, K. T. Short, A. M. Mujsce, and R. A. Rietman, *Phys. Rev. Lett.* **58**, 2333 (1987); D. L. C. Borune *et al.*, *Phys. Rev. Lett.* **58**, 2337 (1987); B. Batlogg *et al.*, *Phys. Rev. Lett.* **59**, 912 (1987); T. A. Faltens *et al.*, *Phys. Rev. Lett.* **59**, 915 (1987).
62. G. N. Subbanna, P. Ganguly, and C. N. R. Rao, *Mod. Phys. Lett. B* **1**, 155 (1987).
63. Y. Matsui, E. T. Muromachi, A. Ono, S. Horiuchi, and K. Kato, *Japan J. Appl. Phys.* **26**, L777 (1987).
64. B. Raveau, C. Michel, and M. Hervieu, *ACS Symp. Ser.* **351**, Chap. 13 (1987).
65. R. A. Camps, J. E. Evetts, B. A. Glowacki, S. B. Newcomb, R. E. Somekh, and W. M. Stobbs, *Nature (London)* **329**, 229 (1987).
66. A. K. Gupta, B. Jayaram, S. K. Agarwal, A. Gupta, and A. V. Narlikar, *Phase Transitions* **10**, 29 (1987).
67. S. V. Bhat, P. Ganguly, T. V. Ramakrishnan, and C. N. R. Rao, *J. Phys. C* **20**, L559 (1987).
68. V. Bhat, A. K. Ganguli, K. S. Nanjunda Swamy, R. A. Mohan Ram, J. Gopalakrishnan, and C. N. R. Rao, *Phase Transitions* **10**, 87 (1987); S. Davison, K. Smith, Y. C. Zhang, J. H. Liu, R. Kershaw, K. Dwight, P. H. Rieger, and A. Wold, *ACS Symp. Ser.* **351**, Chap. 7 (1987).
69. C. N. R. Rao and J. Gopalakrishnan, *Acc. Chem. Res.* **20**, 228 (1987).
70. I. K. Gopalakrishnan, J. V. Yakhmi, and R. M. Iyer, *Nature (London)* **327**, 604 (1987); D. N. Mathews, A. Bailey, R. A. Vaile, G. J. Russell, and K. N. R. Taylor, *Nature (London)* **328**, 786 (1987).
71. R. N. Bhargava, S. P. Herko, and W. N. Osborne, *Phys. Rev. Lett.* **59**, 1468 (1987).
72. M. Zhang, C. Qiang, S. Dakun, J. Rong-Fu, Q. Zheng-Hao, Y. Zheng, and J. F. Scott, to be published.
73. F. Hotzberg, D. L. Kaiser, B. A. Scott, T. R. McGuire, T. N. Jackson, A. Kleinsasser, and S. Tozer, *ACS Symp. Ser.* **351**, Chap. 8 (1987).
74. C. N. R. Rao and J. M. Thomas, *Acc. Chem. Res.* **18**, 113 (1985).
75. D. R. Clark, *Int. J. Mod. Phys. B* **1**, 170 (1987).
76. R. S. Roth *et al.*, *Adv. Ceram. Mater.* **2**, 303 (1987).
77. Ayyub *et al.*, *J. Phys. C* **20**, L673 (1987).
78. J. Narayan *et al.*, *Appl. Phys. Lett.* **51**, 941 (1987).
79. T. Laegreid, K. Fossheim, E. Sandvold, and S. Julsrud, *Nature*, in press.
80. L. Ganapathi, A. K. Ganguli, R. A. Mohan Ram, and C. N. R. Rao, *J. Solid State Chem.*, in press.
81. C. Michel *et al.*, *Z. Phys. B* **68**, 421 (1987).